Dissertation zur Erlangung des Doktorgrades

der Fakultät für Chemie und Pharmazie

der Ludwig-Maximilians-Universität München

The interaction of slug and actin in the DNA double-strand break repair and validation of AI designed potential actin binding compounds for drug discovery

Ling Zhuo

aus Chengdu, Sichuan, P.R.China

2023

Erklärung

Diese Dissertation wurde im Sinne von §7 der Promotionsordnung vom 28. November 2011 von Herrn Prof. Dr. Stefan Zahler betreut.

Eidesstattliche Versicherung

Diese Dissertation wurde eigenständig und ohne unerlaubte Hilfe erarbeitet.

München, den 06.06.2023

Ling Zhuo
_____

Ling Zhuo

Dissertation eingereicht am:	20.06.2023
1. Gutachter:	Prof. Dr. Stefan Zahler
2. Gutachter:	Prof. Dr. Angelika M. Vollmar
Mündliche Prüfung am:	18.07.2023

To my family

Contents

Abstract

1. Abstract

1.1 The interaction of slug and actin in the DNA double-strand break repair process

Introduction

Actin is a protein of central importance for many cellular functions. Its localization and activity are regulated by interactions with a high number of actin binding proteins. In a yeast two-hybrid (Y2H) screening system, the transcriptional regulator snail family transcriptional repressor 2 (SNAI2 or slug) was identified as a potential actin binding protein. The function of the interaction between slug and actin is unclear to date. Since both proteins have been reported to be involved in DNA double-strand break (DSB) repair, we focused on their interaction during this process.

Method

The Matchmaker Gold Y2H system was used to screen for interaction partners of actin. Actin was cloned into the pGBKT7 bait vector, and subsequently introduced into the Y2H Gold reporter strain, which was then mated with the Mate&Plate™ library – Universal Human in yeast strain Y187. The interaction between slug and actin was further confirmed by co-immunoprecipitation experiments in Hela cells. Actin polymerization was modulated by jasplakinolide and latrunculin B with 20nM and 100nM, slug levels were detected by Western blot and immunofluorescence. To expand the analysis of this interaction, immunofluorescence was performed to visualize the actin morphology after slug silencing with siRNA and overexpression with SlugMyc_pcDNA3 plasmid. Combination treatments were implemented through pretreatment with actin binding agents for 1 h and coupled with the induction of DNA damage (via doxorubicin or UV exposure), the apoptosis was measured by flow cytometry. To investigate the role of the interaction in DSBs process, the relationship between nuclear actin, slug and two DNA damage factors (γ-H2AX and RPA2) were

evaluated by immunofluorescence and subsequent confocal microscopy (analysis of co-localization). Treatment with 250nM doxorubicin for 2 h was used to induce DNA damage. All experiments were performed as independent triplicates.

Results

We identified several proteins in the Y2H screening system: some known actin binding proteins, like cofilin 2 (CFL2), or cyclase associated actin cytoskeleton regulatory protein 1 (CAP1), as well as previously unknown interactors like NLRP1, LAMTOR5 and slug. Co-immunoprecipitation experiments confirmed the interaction between slug and actin. Manipulation of actin polymerization diminished slug intensity by 30 percent in the nucleus and silencing of slug induced cytosolic actin filament aggregation showing the rise of particle count of cytoskeleton from 2 (non-targeting) to 25 (siSlug). Combination treatment with actin binding agents synergistically enhanced cell apoptosis after DNA damage (evoked by 250nM doxorubicin or 150 s UV-irradiation). Slug could bind to nuclear actin (Pearson correlation coefficient value: r>0.3). Nuclear actin overexpression promoted slug recruiting to damage foci and repair site (increase of the Pearson correlation coefficient value from 0.23 to 0.42) and mediated the co-localization between slug and DNA damage repair factors (P≈0.036[*]).

Conclusions

Slug is a novel actin binding protein and could bind to nuclear actin. The combination of targeting actin and DNA damage synergistically enhanced cell apoptosis. The interaction of slug and nuclear actin might be involved in the DNA double-strand break repair process.

1.2 Validation of AI designed potential actin binding compounds for drug discovery

Introduction

High-throughput screening (HTS) is an essential part of the current drug discovery process, and is able to screen billions of synthesizable molecules from massive chemical libraries against biological targets in days. However, artificial intelligence (AI) technology provides the competitive advantages of speed and scale. The AtomNet® screening system deep learning-based approaches, developed by the company Aromwise, conduct the extensive application of machine learning to drug discovery. Once a lead molecule has been identified by the AtomNet® convolutional neural network, additional testing is required to characterize lead compounds further and assess their potential efficacy. In addition, the molecules selected by the company are novel drug-like scaffolds rather than minor modifications to known bioactive compounds. In collaboration with Atomwise, we aimed to validate compounds predicted to be actin binders in vitro and in cellular assays.

Method

First, compounds were tested for their capability to modulate actin polymerization by pyrene assay. Pyrene fluorescence was monitored every 20 s in a 96-well fluorescence plate reader (Infinite® 200 PRO) at 360 nm excitation and 400 nm emission wavelength. Then, Hela cells (cervical cancer cells) were treated with indicated concentrations (3μM, 10μM, 30μM, 100μM, 200μM) respectively for 72 h. Cells were stained with crystal violet and measured with spectrophotometer at 550 nm. Cell viability was quantified and IC50 value was calculated. Next, confluent cells were scratched and treated with the same setting of concentrations with above experiment for 24 h, and the relative wound area was quantified to evaluate the influence on cell migration. Finally, Hela cells were incubated with 200μM of selected compounds for 24 h and actin morphology was visualized by confocal microscopy. All experiments were performed as independent triplicates.

Results

First of all, we screened out seven target compounds from the first-generation candidates (83 compounds) as in vitro actin polymerization inhibitors. After that, the second-generation candidates (102 compounds) were synthesized based on the structural modification of the seven selected compounds, and one target was screened out by the same method. Due to solubility issues, only six compounds were finally used in the following cellular experiments. On the one hand, all the six compounds could inhibit Hela cell proliferation and migration to a certain extent. On the other hand, some compounds disrupted the distribution of cytoskeleton. In particular, compound2 and compound5 showed the correlation with the absence of cytoskeleton and accumulation of actin around the nucleus.

Conclusions

Six available screened out actin polymerization inhibiting compounds were validated in Hela cells. High concentrations of the compounds inhibited Hela proliferation and migration significantly. The actin cytoskeleton was impaired significantly after compound2 and compound5 treatment for 24 h. The selected compounds had the desired effects in Hela cells to a certain degree, but need to be improved concerning potency in further studies. We have the proof of principle that the AtomNet® screening system works in finding novel actin binding compounds. Thus, it is worth considering the further structural modification of the screened compounds to enhance the binding to actin and to improve the anti-tumor effects in cellular assays.

Introduction

2. Introduction

2.1 Involvement of actin dynamics in cellular function

The evolutionarily ancient, highly conserved actin molecule can assemble reversibly into filaments, which form dynamic networks called actin cytoskeleton in the cell cytoplasm [1]. The highly dynamic and versatile actin reorganization is involved in a wide range of cellular functions, including: cell shape and mechanical support, cell invasion and metastasis, intracellular transport and cell-cell interactions. The machinery of these processes relies on high sensitivity of the actin cytoskeleton to the cellular environment [2].

The eukaryotic actin polypeptide is composed of 375 amino acid residues, and a folding pattern is formed into a globular protein structure, named G-actin. This monomeric form of actin (**Figure 2-2.1 A**) has a unique shape that resembles a twisted double-stranded helix with four subdomains and the central ATP-binding pocket, which forms a structure with a deep crack or cleft-like region [3]. The subdomain 2 of actin, and in particular its DNase-I binding loop, are the most dynamic elements to influence actin-based processes. The displacement loop (D-loop) provides a unique binding site allowing for specific interactions and functional regulation [4, 5].

Furthermore, G-actin has an increased ability to participate in actin filament formation when adenosine triphosphate (ATP) is bound to it. Meanwhile, G-actin can also undergo ATP hydrolysis to adenosine diphosphate (ADP) and inorganic phosphate (Pi), resulting in a conformational change which strongly interferes with the dynamic regulation of actin within cells [6, 7]. The hydrolysis of ATP triggers G-actin monomers assembling into long, helical filaments known as F-actin [8]. The transition of actin is called elongation or polymerization. Pyrene is a sensitive fluorescent compound that can be used as a probe to study this process, and the measurements

do not influence actin kinetics. Therefore, pyrene assay has been extensively used to investigate actin polymerization [9] (**Figure 2-2.1 B**).

Actin dynamics refers to the complex processes involved in the assembly, disassembly, and reorganization of actin filaments within cells. These processes are regulated by actin nucleating proteins such as the Arp2/3 complex and formins. Actin filaments can depolymerize by losing G-actin subunits from their ends, and this dynamic change is regulated by ABPs like cofilin [10, 11]. Actin filaments play essential roles in various cellular functions. For example, their assembly and organization contribute to maintaining cell shape and providing mechanical support to cells [12]. Moreover, actin filaments aggregate at the leading edge of migrating cells to allow cells to move and migrate in response to various signals [13]. Additionally, because filaments can act as scaffolds for signaling molecules, actin dynamics is involved in cellular sensing and signal transduction [14]. In short, the precise regulation of actin dynamics is essential for proper cellular function and response to environmental cues.
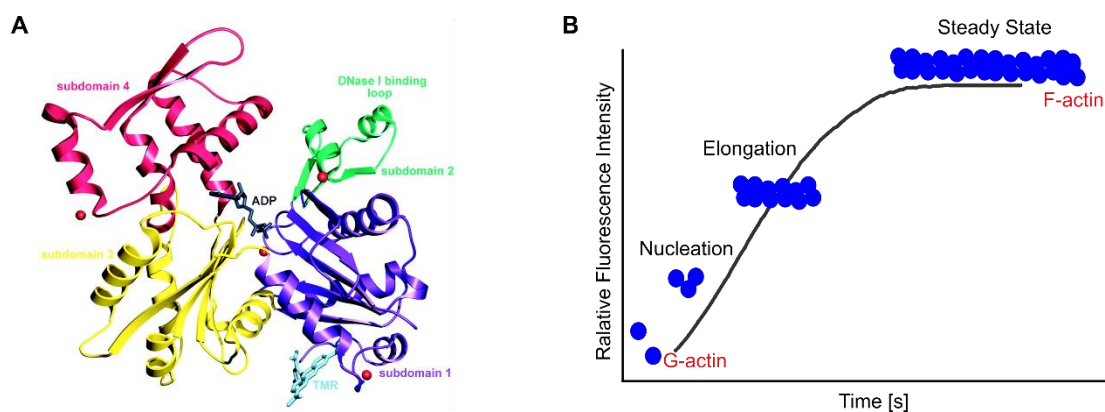
Figure 2-2.1 Actin structure and actin polymerization.
(A) Crystal structure of actin monomer in the ADP state. Actin subdomains are represented in different colors: subdomains 1 (purple), 2 (green), 3 (yellow), and 4 (red). The nucleotide rearrangement of the DNase-I-binding loop (green) dependents crystal structure of uncomplexed G-actin in the ADP state. The molecule used to prevent actin polymerization (TMR) (cyan) during crystallization is covalently bound near the C-terminus [15].
(B) Actin polymerization curve. A schematic model of the pyrene polymerization assay. Pyrene fluorescence increases upon incorporation into actin filaments, providing a quantitative measure of actin polymerization.

2.2 Actin and actin binding protein in the nucleus

Both nuclear localization sequence (NLS) and nuclear export signal (NES) sequences are specific sequence motifs found in proteins and recognized by specific transport receptors. NLS acts as a signal for the nuclear import machinery that facilitates proteins transport into the nucleus, and NES is found in proteins that regulates their localization from the nucleus to the cytoplasm [16-18].

The nuclear translocation of actin in response to certain types of stress conditions, including heat shock and dimethyl sulfoxide (DMSO) treatment, may be linked to two NES sequences [19, 20]. And disruption of the NES in actin mutants might cause aberrant accumulation of actin in the nucleus, leading to abnormal localization and affecting the balance of nuclear processes and ultimately impacting cell proliferation. However, actin has no NLS, the nuclear localization of actin is facilitated by NLS sequences present in actin binding proteins (ABPs) [20]. These ABPs can interact with actin monomers or actin filaments and contain NLS motifs that allow them to be imported into the nucleus. Once inside the nucleus, actin and its associated proteins can participate in nuclear processes, contributing to the regulation of gene expression and nuclear architecture [21].

In cells, the organization of actin filaments and actin dynamics are regulated by a large amount of ABPs [22]. This diverse group of proteins are classified into different types, for instance, monomer-binding proteins, capping proteins, severing proteins, cross-linking proteins, etc. [23]. Profilin is a small, highly conserved protein which is early detected as an actin monomer-binding protein. It enhances the availability of actin monomers for filament assembly by promoting nucleotide exchange [24]. Another widely concerned actin binding protein is cofilin, the phosphorylation of it by specific kinases can either activate or inhibit its depolymerizing activity, thereby modulating actin dynamics [25]. Besides, fimbrin is an actin binding protein that is

responsible for bundling actin filaments. These bundled structures contribute to the stability and mechanical properties of the actin cytoskeleton [26].

Currently, more and more proteins involved in actin filament formation and function are found in the nucleus (**Table 2-1**). Initially, actin and actin-related proteins (ARPs) were predominantly associated with their roles in the cytoplasm. However, research over the past decade has revealed that these proteins are also functional within the nucleus. By being present in the nucleus, actin can interact with other nuclear proteins and complexes to modulate various nuclear processes such as gene expression regulation [27], chromatin remodeling [28], and DNA repair [29]. These proteins contribute to the dynamic organization and structural integrity of the nuclear compartment, similar to their roles in the cytoplasm [30]. The exact mechanisms by which actin and actin-associated proteins exert their functions in the nucleus are still under investigation.

Protein	Function
Profilin	A monomer-binding protein that promotes nucleotide exchange
CapG	An abundant protein in macrophages, which binds pointed ends of F-actin
Zyxin	Zyxin organizes the actin-polymerization machinery and has actin-polymerization-promoting activity
Myopodin	A filamentous (F)-actin-bundling protein
Nrf2	On oxidative stress, it forms a complex that trans-locates to the nucleus
NDHII	A helicase that seems to bind a form of F-actin in the nucleus
Emerin	A nuclear-envelope protein that interacts with lamin A and actin
Lamin A	A major protein of the nuclear lamina, which binds nuclear actin
Exportin-6	A nuclear-export receptor that specifically exports profilin-bound actin
DBP40,hrp36,hrp65	Proteins that associate with pre-mRNA to form ribonucleoprotein complexes

Table 2-1 Identified actin binding proteins in the nucleus [31].

2.3 Nuclear actin and actin related proteins in DNA double-strand break repair

DNA double-strand breaks (DSBs) are severe types of DNA damage that can arise from various sources, including ionizing radiation, reactive oxygen species, and certain chemicals, like doxorubicin [32]. When DNA damage forms DSBs, the histone variant H2AX undergoes phosphorylation at the serine 139 residue near the site of the DNA damage. This phosphorylated form is known as gamma H2AX or γ-H2AX and can be used as a biomarker for damage [33]. Cells have evolved several pathways to repair DSBs, with the two major pathways being homologous recombination (HR) and non-homologous end joining (NHEJ) [34, 35] (**Figure 2-2.2**).

HR is a high-fidelity repair pathway that primarily operates during the S and G2 phases of the cell cycle. The DSB ends are processed by nucleases to generate 3' single-stranded DNA (ssDNA). The emergent tail is rapidly coated by replication protein A (RPA) to limit spurious interactions with ssDNA intermediates of other nuclear processes. Breast cancer type 2 susceptibility protein (BRCA2) mediates the replacement of RPA by RAD51, to form a nucleoprotein filament that arches for the homologous sequence on the sister chromatid and forms a D-loop structure. The invading strand uses the intact sister chromatid as a template for DNA synthesis [36]. Altered HR (homologous recombination) genes are commonly found in several types of cancer, including breast, ovarian, and pancreatic cancer. HR proteins play crucial roles in DNA repair, particularly in repairing double-strand DNA breaks, and their dysregulation contributes to tumorigenesis and therapeutic resistance. As a result, HR proteins have emerged as prospective targets for cancer therapeutics [37].

NHEJ is an error-prone repair pathway that operates throughout the cell cycle. Ku70/Ku80 bind to the DNA ends and recruit DNA-PKcs to process the ends. The processed DNA ends are aligned, allowing DNA ligase IV to ligate them together. In some cases, NHEJ repair may require that the ends can be trimmed by nucleases

(such as Artemis) [38]. Cancer cells often exhibit alterations in the NHEJ pathway, leading to aberrant DNA repair and genomic instability. Combined NHEJ pathway inhibitors with DNA-damaging agents, such as chemotherapy or radiation therapy, can enhance their effectiveness [39, 40]. Targeting this pathway can be a valuable strategy for cancer therapeutics.
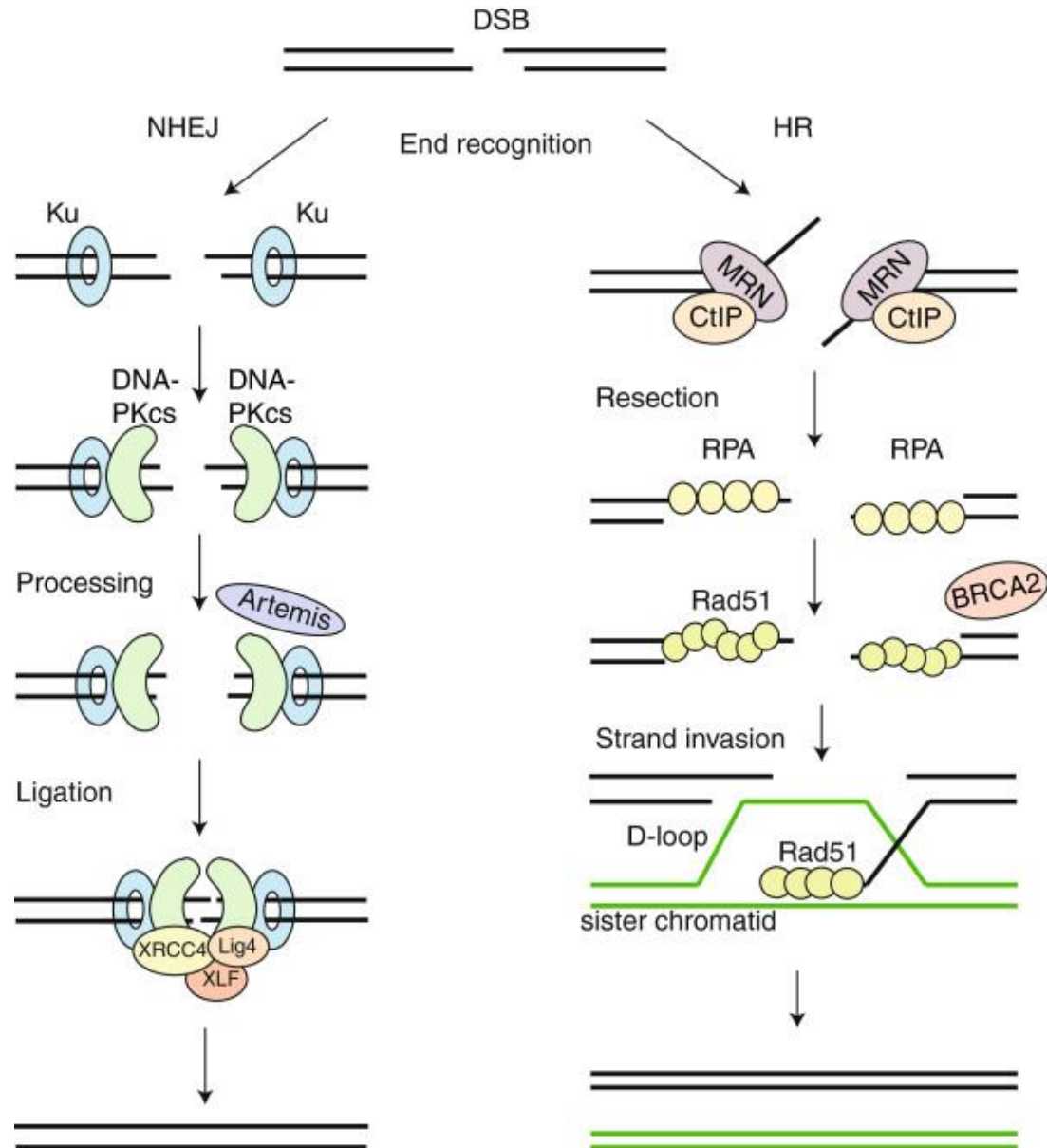
Figure 2-2.2 The two major pathways of DNA double-strand break repair.
DSBs are predominantly repaired by either an error-prone pathway-non-homologous end joining (NHEJ), or an error free pathway-homologous recombination (HR) [41].

Actin has been implicated in the cellular response to DNA damage and repair. Recent research has indeed provided evidence for a requirement of polymerized actin in DNA DSB repair. The results of the experiment demonstrated that the recruitment of Ku80-GFP at sites of UV damage decreases under two conditions: actin depolymerization induced by cytochalasin D and the presence of polymerization-incompetent NLS-G13R actin. This suggests that actin dynamics and polymerization play a role in Ku80 retention at sites of DNA damage [42]. Additionally, nuclear actin binding proteins (NABPs) mediate the interaction between actin filaments and other nuclear proteins, contributing to the coordination and regulation of DNA damage signaling and repair pathways. These proteins are components of chromatin remodeling complexes, such as actin-related protein (ARP) family, which interact with nuclear actin and modulate its functions during DNA damage response [29]. This study has shown that that the ARP2/3 complex is recruited to DSBs and contributes to their clustering in the nucleus. The actin filaments nucleated by ARP2/3 can physically link different DSBs together, bringing them into close proximity. This clustering of DSBs is thought to enhance the efficiency of HD repair by increasing the chances of homologous DNA template encounter [43].

2.4 The role of slug in the DNA damage repair process

Slug, also known as SNAI2, is a protein that plays a crucial role in embryonic development and tissue formation. It belongs to the Snail family of transcription factors [44], which are involved in regulating gene expression during development [45], cell differentiation [46], and cancer progression [47]. Slug is primarily known for its role in epithelial-mesenchymal transition (EMT), a process in which epithelial cells acquire mesenchymal characteristics. EMT is essential for embryonic development and wound healing, but it can also contribute to cancer metastasis when deregulated [48, 49].

In recent years, there has been increasing attention to the issue of how slug is involved in DNA damage repair (DDR). Upon DNA damage, p53 is activated and acts as a transcription factor, regulating the expression of various target genes involved in DNA repair pathways, such as nucleotide excision repair (NER) [50], base excision repair (BER) [51], and DSBs [52]. Slug can directly bind to the p53-responsive elements in the promoter regions of target genes and prevent p53 from activating their transcription [45]. Moreover, some studies have shown that the abnormal expression of slug leads to a decrease in the expression of p53 target genes involved in DNA repair [53]. Some experiments have been conducted to study the function and role of slug in DSB repair and DNA damage response (DDR) signaling cascade. By examining γ-H2AX and RPA32 proteins in slug-deficient cells, persistence of unresolved DNA damage elucidates the contribution of slug in efficient DSB repair processes [54]. As all these events are associated with the DNA damage process to which deficiency of slug, it can reasonably be assumed that slug is necessary for effective DDR, but the mechanisms of the direct involvement of slug in DNA damage resolution has not been in-depth studied at present.

2.5 The potential of actin binding compounds for clinical cancer therapy

The major types of building blocks of the actin cytoskeleton are actin filaments, microtubules and intermediate filaments. The reversible assembly of actin microfilaments allow the cytoskeleton to adapt and remodel in response to cytoskeletal mechanical support and biological movements of cells [55]. Microtubules are much stiffer than actin filaments, the presence of GTP-bound tubulin promotes their assembly as needed for intracellular transports and maintaining the polarized organization of cells [56]. Intermediate filaments are homopolymeres or heteropolymeres consisting of a diverse group of monomeric proteins. Unlike the above two components, intermediate filaments are more stable and less dynamic and are able to reinforce cell-cell-adhesion [57]. Of these cytoskeletal components, actin have a notably rich diversity of structure and function.

Actin binding compounds play a significant role in modulating the cytoskeleton. By targeting actin and modulating its dynamics, actin binding compounds provide a valuable tool for studying the cytoskeleton's role in cellular processes and disease states [58]. They are used extensively in research to investigate cytoskeletal functions, cellular mechanics, and the mechanisms underlying various diseases, including cancer [59], neurodegenerative disorders [60], and cardiovascular diseases [61].

Latrunculin B is a natural compound derived from the red sea sponge Latrunculia magnifica. It is a potent actin binding compound that disrupts actin dynamics by specifically binding to actin monomers and preventing their incorporation into actin filaments, thereby inhibiting actin polymerization [62]. Another natural compound originally isolated from marine sponges is jasplakinolide, which stabilizes actin filaments and leads to the formation of thicker and more stable actin structures. Jasplakinolide is often used in combination with fluorescent dyes to stain actin in

fixed cells for imaging studies [63]. Chondramides can bind to actin filaments and disrupt their function. They have been found to inhibit cancer cell migration and invasion and have been studied for their potential in cancer therapy, particularly in the context of metastasis [59].

It's important to note that the development of actin binding compounds for clinical cancer therapy is still in the early stages, their specific mechanisms of action and potential side effects need to be further characterized. Clinical trials and ongoing research will help determine the potential of these compounds for cancer treatment. While these compounds show promise, further research is needed to fully assess their efficacy in animal models and clinical trials, and evaluate their safety and efficacy.

2.6 Atomwise company and AtomNet® technology

The process of discovering and developing a new medicine can be costly and time-consuming. The rising costs and extended timelines in drug development are well-recognized challenges in the pharmaceutical industry [64]. To address these challenges, artificial intelligence (AI) and machine learning (ML) are used to streamline and accelerate drug discovery and development. These technologies have the potential to optimize target selection, improve virtual screening and predictive modeling, enhance clinical trial design [65].

Atomwise is a biotechnology company which utilizes deep learning algorithms and analysis of vast amounts of data to predict the binding affinity between small molecules and target proteins [66]. The AtomNet® platform is built with industry-leading tools for AI and ML technology that enable massive scale screening with unprecedented speed and discover small molecule drugs more efficiently than traditional approaches to deliver better medicines, faster. Specifically, Atomwise approach involves using a convolutional neural network, which are commonly employed in image recognition tasks, to analyze molecular structures and predict their properties or interactions [67]. By training their deep learning models on large datasets of molecular structures and their associated biological activities, AtomNet® can generate predictive models that assist medicinal chemists in drug discovery. These models can predict properties such as binding affinity, selectivity, and toxicity, allowing researchers to prioritize and optimize the design of potential drug candidates [68].

To identify some novel, druggable inhibitors of actin, a virtual screening campaign for actin was conducted by Atomwise. Kabiramide (KAB) is a natural compound that has been identified as an actin polymerization inhibitor, the formation of the complex between kabiramide C (KABC) and actin was shown to regulate actin filament dynamics [69]. Besides, KABC and related macrolides are useful probes to study the

regulation of the actin filament (+) end [70]. Therefore, the KAB was used to be a bound ligand in the screening, the interaction site of it could be a scaffold to find small molecules with a similar binding mode. The crystal structure (**Figure 2-2.3**) for actin (PDB code: 4K41) contains KAB, that marks the binding site for use with AtomNet®. Subsequently, Atomwise screened a molecular library of several million compounds at the selected target site using its proprietary technology. Top scoring compounds were clustered and filtered to arrive at a final subset of deliverable compounds.
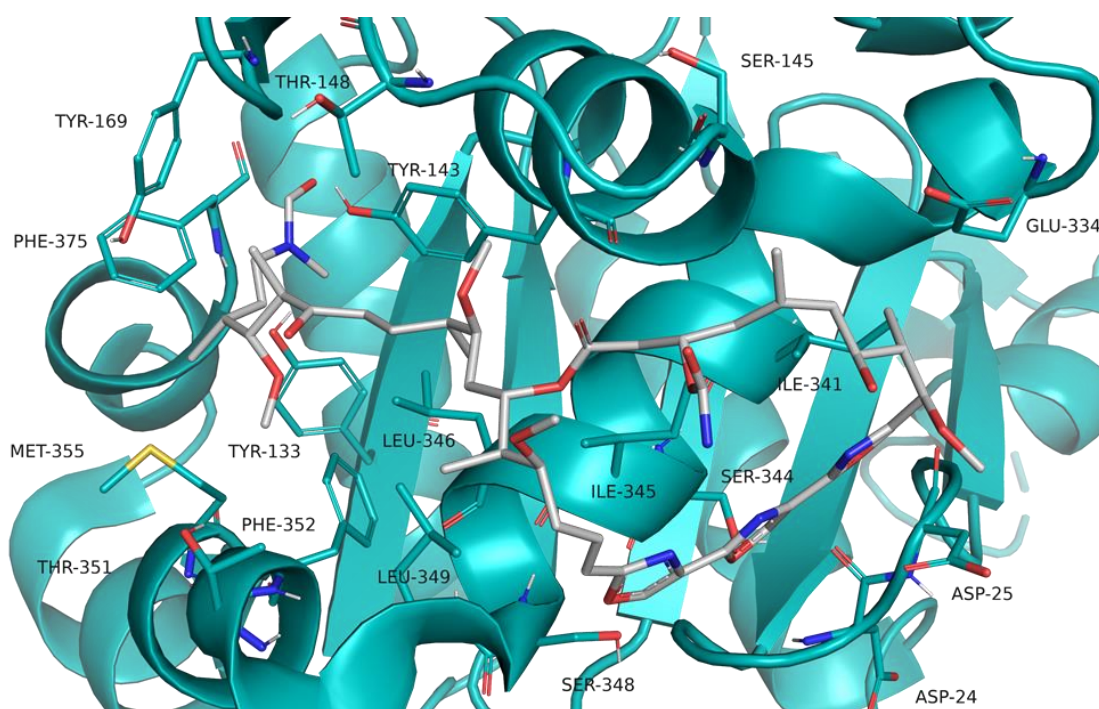
Figure 2-2.3 The graphic representation of the AtomNet® designed crystal structure. The surface around the proposed binding-site with KAB (grey) bound and the residues that encompass the binding site.

2.7 Aims of the study

Regarding the powerful capabilities of actin and actin-targeting therapies are still in the early stages, we aimed to explore the functional relationship between slug and actin in the context of DNA double-strand break repair and investigate efficacious AI designed actin binding compounds for clinical application.

Part I:

The interaction of slug and actin in the DNA double-strand break repair

1. Verify the interaction between slug and actin

2. Manipulation of slug or actin and study the impact on each other

3. Validate the role of slug in DNA double strand break pathway

4. Determine the relationship of slug and actin in DNA damage in the nucleus

5. Explore the interaction between slug and actin in DNA double strand break

Part II:

Validation of AI designed potential actin binding compounds for drug discovery

1. Screen out potential actin binding compounds

2. Functional characterization of the selected compounds in Hela cells concerning proliferation and wound healing

3. Reveal the preliminary mechanism of the compounds on cells by observing the cytoskeleton structure

Materials and Methods

3. Materials and Methods

3.1 Materials

3.1.1 Technical equipments

Device	Producer
ChemiDoc™ Touch Imaging System	Bio-Rad Laboratories, Munich, DE
Digital block heater HX-1	Peqlab, Wilmington, USA
Electrophoresis Power Supply	Bio-Rad Laboratories, Munich, DE
FACSCanto™ II	BD Biosciences, Heidelberg, DE
HERACell 150i incubator	Thermo Scientific, Waltham, USA
Infinite® 200 PRO microplate reader	Tecan, Crailsheim, DE
Leica TCS SP8 confocal microscope	Leica Microsystems, Wetzlar, DE
Mikro 22R/220R centrifuge	Hettich, Tuttlingen, DE
Nanodrop® Spectrophotometer	Peqlab, Wilmington, USA
Optima™ MAX-XP ultracentrifuge	Beckman Coulter, California, USA
Primus 25 advanced® Thermocycler	Peqlab Biotechnologie, Linz, AT
QIAamplifier 96	QIAGEN, Hilden, DE
SpectraFluor Plus microplate reader	Tecan, Grodig, AT
Thermoshake incubator shaker	Gerhardt, Koenigswinter, DE
Unitwist 300 orbital shaker	IKA, Staufen, DE
Vi-Cell™ XR cell counter	Beckman Coulter, Fullerton, USA
Water bath Haake W19	Thermo Scientific, Waltham, USA

Table 3-1 Technical equipments

3.1.2 Compounds

The screening actin binding compounds for cell biology testing in the project were supplied by Atomwise company, Inc. (CA, USA) as part of the Artificial Intelligence Molecular Screen (AIMS) awards program through Mcule, Inc. (CA, USA). All compounds were stored at -20 °C after dissolution. For cellular experiments, they were further diluted in cell growth medium with a maximum end concentration of

dilution reagent of 0.1% (v/v). Doxorubicin was diluted in ddH2O, latrunculin B and

jasplakinolide were diluted in DMSO.

Compound	Producer
Doxorubicin hydrochloride	Merck, Darmstadt, DE
Latrunculin B (ab144291)	Abcam, Cambridge, UK
Jasplakinolide 97% (HPLC)	Sigma-Aldrich, Taufkirchen, DE

Table 3-2 Compounds

3.1.3 Chemicals and reagents

The following table (3-3.1) contains a list of all chemicals and reagents used in this

study. Antibodies (3-3.2, 3-3.3) and plasmids (3-3.4) are listed separately.

Chemical and Reagent	Producer
16% FormalDEhyDE Solution, Methanol-free	Thermo Fisher, Waltham, USA
Ammonium persulfate (APS)	Merck, Darmstadt, DE
Ampicillin	ThermoFisher, Waltham, USA
Bovine serum albumin (BSA)	Sigma-Aldrich, Taufkirchen, DE
Bradford reagent Roti® Quant	Bio-Rad, Munich, DE
Collagen G	Biochrom AG, Berlin, DE
Competent DH5α-E. coli	New England BioLabs, Frankfurt, DE
Complete®	Roche Diagnostics, Penzberg, DE
Coumaric acid	Merck, Darmstadt, DE
Crystal Violet	Carl Roth, Karlsruhe, DE
DharmaFECT™ Transfection reagents	Horizon Discovery, Cambridge, UK
Dimethyl sulfoxide (DMSO)	Carl Roth, Karlsruhe, DE
Dithiothreitol (DTT)	Sigma-Aldrich, Taufkirchen, DE
Dulbecco's Modified Eagle Medium (DMEM)	Anprotec, Bruckberg, DE
ECL Plus WB detection reagent	GE Healthcare, Munich, DE
Ethylendiaminetetraacetic acid (EDTA)	Sigma-Aldrich, Taufkirchen, DE
FastDigest restriction enzymes and buffer	Thermo Fisher, Waltham, USA
Fetal calf serum (FCS)	Anprotec, Bruckberg, DE
FluorSave® reagent mounting medium	Merck, Darmstadt, DE
GeneRuler 1 kb Plus DNA ladder	Thermo Fisher, Waltham, USA
Glycerol	Applichem, Darmstadt, DE
Invitrogen™ LB Agar, powder	Thermo Fisher, Waltham, USA
Invitrogen™ LB Broth Base	Thermo Fisher, Waltham, USA
Lipofectamine™ 3000 transfection reagent	ThermoFisher, Waltham, USA
Luminol	AppliChem, Darmstadt, DE
$MgCl_2$	AppliChem, Darmstadt, DE
NaCl	Carl Roth, Karlsruhe, DE
Page Ruler™ Prestained Protein Ladder	Thermo Fisher, Waltham, USA
Primers	Metabion, Planegg, DE
Pyrene Actin 10% (rabbit skeletal muscle)	Hypermol, Bielefeld, DE
Sodium dodecyl sulfate (SDS)	Carl Roth, Karlsruhe, DE
TEMED	Carl Roth, Karlsruhe, DE
Thiazolyl Blue Tetrazolium Bromide (MTT)	Avantor, Pennsylvania, USA
Tris-Base	Sigma-Aldrich, Taufkirchen, DE
Triton X-100	Merck, Darmstadt, DE
Trypsin	PAN Biotech, AiDEnbach, DE
Tween 20	Sigma-Aldrich, Taufkirchen, DE

Table 3-3.1 Chemicals and reagents

Primary Antibody	Producer
Anti-RPA32/RPA2 antibody	Abcam, Cambridge, UK
mCherry Polyclonal antibody	Proteintech, Planegg, DE
Monoclonal Anti-ACTB antibody	Sigma-Aldrich, Taufkirchen, DE
Phospho-Histone H2A.X (Ser139) mAb	Cell Signaling Technology, Danvers, USA
Slug (C19G7) Rabbit mAb	Cell Signaling Technology, Danvers, USA

Table 3-3.2 Primary antibody

All the secondary antibodies were purchased from Thermo Fisher, Waltham, USA.

Secondary Antibody
Goat anti-Rabbit IgG (H+L) Cross-Adsorbed Secondary Antibody, Alexa Fluor 488
Goat anti-Rabbit IgG (H+L) Highly Cross-Adsorbed Secondary Antibody, Alexa Fluor 546
Goat anti-Mouse IgG (H+L) Highly Cross-Adsorbed Secondary Antibody, Alexa Fluor 633

Table 3-3.3 Secondary antibody

Plasmid	Producer
Nuclear Actin-Chromobody® plasmid	ChromoTek acg-n
pCAG-mGFP-Actin	Addgene #21948
pmCherry-C1 actin-3XNLS P2A mCherry	Addgene #58475
pcDNA3-EGFP	Addgene #13031
SlugMyc_pcDNA3	Addgene #31698

Table 3-3.4 Plasmids

3.1.4 Consumbles

Consumables	Producer
96-well half area black fLat Bottom microplate	Corning Incorparated, New York, USA
Amersham™ PVDF membrane (0.45 µM)	Merck, Darmstadt, DE
Cell culture flask: T25/T75	Sarstedt, Nuembrecht, DE
Cover slip (8 × 8 mm)	H.Saur Laborbedarf, Reutlingen, DE
Disposable pipette: 5/10/25 ml	Greiner Bio, Frickenhausen, DE
FACS tube: 5 ml	Sarstedt, Nuembrecht, DE
Falcon tube: 15/50 ml	VWR, Bruchsal, DE

Microcentrifuge Tube: 1.5ml	Beckman Coulter, Krefeld, DE
Microtiter plates: 6/12/96 well	Greiner Bio, Frickenhausen, DE
Microtube: 1.5 ml, black	Carl Roth, Karlsruhe, DE
Microtube: 1.5 ml, brown	Sarstedt, Nuembrecht, DE
Pipette tips: 10/100 µl/1000 µl	Sarstedt, Nuembrecht, DE
Research plus™ Adjustable Volume Pipette	Eppendorf, Hamburg, DE
Safe-Lock Tube: 0.5/1.5 ml	Eppendorf, Hamburg, DE
µ-Slide 8 well	Ibidi GmbH, Munich, DE

Table 3-4 Consumbles

3.2 Methods

3.2.1 Cell culture

Hela cells in this study were from DSMZ (Leibniz Institute, Braunschweig, Germany). Cells were cultured in DMEM supplemented with 10% fetal bovine serum (FBS) and incubated at 37 °C, 95% humidity with 5% CO_2.

Buffer and Solution	Component	Content
PBS (pH 7.4)	Nacl	132.2mM
	Na_2HPO_4	10.4mM
	KH_2PO_4	3.2mM
	H_2O	
Trypsin-EDTA	Trypsin	0.05%
	EDTA	0.20%
	PBS	
Growth medium	DMEM	500 ml
	FCS	50 ml
Freezing medium	FCS	90%
	DMSO	10%
Collgen G	Collagen G	1.25 ml
	PBS	500 ml

Table 3-5 Cell culture buffers and solutions

3.2.1.1 Passaging

When cells reached confluency, the growth medium was removed and cells were gently rinsed with pre-warmed PBS. After 1 min incubation with trypsin-EDTA at 37 °C, tryptic digestion was stopped by the addition of standard growth medium. Cells were centrifuged at 1000 rpm for 5 min and the pellet was re-suspended in fresh growth medium. Cell number was counted using a Vi-Cell™ XR cell counter. Cells were split into 75 cm^2 cell culture flasks with desired density or seeded in multiple well plates further experiments. The passaging process was repeated as necessary to maintain cell viability and growth. Cells were used within 40 passages in this study.

3.2.1.2 Freezing and thawing

For long-term cryopreservation, confluent cells were washed with sterile PBS and detached with trypsin-EDTA. Trypsin was inactivated by fresh medium and cells were collected by centrifugation (1000 rpm, 5 min, RT). Then re-suspend cells in 3 ml ice-cold freezing medium. 1.5 ml aliquots were frozen in cryovials and transferred to -80 °C for 24 h before being moved to liquid nitrogen freezer for long-term storage.

In order to thaw cells, cells in cryovials were immediately dissolved in a 37 °C water bath. Once the ice has melted, transfer the cell suspension to a sterile tube, DMSO was removed by centrifugation, cells were re-suspended in 15 ml pre-warmed fresh growth medium and transferred into a 75 cm^2 flask (pre-coated with Collagen G). Cells were incubated in the incubator for growth.

3.2.2 Cloning

Actin was amplified from pCAG-mGFP-Actin plasmid for mammalian expression using the following primers adding BamHI and EcoRI restriction sites:

Primer (5'-3')	Sequence

Forward	CATGGAGGCCGAATTCATGGATGATGATATCGCCGCGCTC
Reverse	GCAGGTCGACGGATCCGAAGCATTTGCGGTGGACGATGGA

Table 3-6 Primers for actin fragment amplification

The PCR products were analyzed with a 1% agarose gel and purified using QIAGEN gel extraction kit. The purified insert and the bait vector pGBKT7 were digested with BamHI and EcoRI. The vector was further dephosphorylated by directly adding 1 µl of FastAP thermosensitive alkaline phosphatase. Vector and insert were again purified using a gel extraction kit. Ligation was carried out in a 1:3 (vector: insert) using the protocol from Thermo Fisher Scientific at RT for 30 min, followed by heat shock transformation of the ligation mixture into chemical competent E. coli DH5-α. Plasmid isolation was performed using the QIAprep® Spin Miniprep Kit. Plasmids were analyzed by PCR and sequencing using a standard T7 primer.

3.2.3 Matchmaker gold yeast two hybrid system screening

The Matchmaker Gold yeast two hybrid system (Takara Bio) was used to screen for interaction partners of actin following the manufacturer's instructions. In brief, the amplified actin was cloned into the pGBKT7 bait vector. The vector was introduced into the Y2H Gold reporter strain, which was then mated with the Mate&Plate™ library – Universal Human (Normalized, Takara Bio) in yeast strain Y187. The screening was performed following the Matchmaker manual. An aliquot was screened (5-fold library coverage) on plates (15 cm diameter) containing DDO/X/A medium. After incubation, 960 blue colonies were picked from the plates, and re-spotted on 10 each of 15 cm diameter plates containing the following media (40 plates in total): DDO, DDO/X/A, QDO, and QDO/X/A. 480 colonies which showed robust growth on all plates, and blue color on both plates containing X-α-Gal were classified as 'hits', and were spotted on DDO plates to ensure robust growth. Then, colony PCR was performed for those colonies. Samples showing a band (even if weak) on an agarose gel were analyzed by sequencing (76 samples with Eurofins

Genomics, 464 samples with Macrogen Europe, both T7 standard sequencing primer, some samples were repeated due to bad sequencing quality). The identity of the insert was revealed using a BLAST search (https://blast.ncbi.nlm.nih.gov/). The colony containing the SNAI2 hit was selected, and the plasmid was isolated (Zymoprep™ Yeast Plasmid Miniprep kit, Zymo Research). SNAI2 was identified once. Cloning and Matchmaker Gold yeast two hybrid screening were conducted by Dr. Simone Moser (Prof. Vollmar, LMU Munich).

3.2.4 Co-Immunoprecipitation

Cells in 6-well were washed with ice-cold PBS for 3 times, and then 100 µl RIPA lysis buffer was added. The plate was incubated on ice for 30 min with occasional shaking. Cells were scrapped off and transferred to 1.5 ml tubes. The cell debris were removed by high-speed centrifugation (10,000 g, 10 min, 4 °C) and the supernatant was collected afterwards. Protein concentration was determined by Bradford assay. 2 µg (1:50) of monoclonal antibody was mixed with the supernatant and 50 µl of µMACS Protein G MicroBeads were added. The lysates were then incubated at 4 °C overnight with shaking. The µColumn was rinsed with 200 µl lysis buffer, and let lysate run through the column. After incubation with the protein solution, the column was rinsed 4x with 200 µl RIPA buffer and with 100 µl low-salt buffer once. After elution, the column was applied with 20 µl of pre-heated SDS-PAGE sample buffer and incubated for 5 min at room temperature. Another 50 µl of pre-heated SDS-PAGE sample buffer was eluted in a fresh 1.5 ml tube. The sample was boiled for 5 min at 95 °C and stored at -20 °C for subsequent western blot verification.

3.2.5 Western blot

3.2.5.1 Sample preparation

For preparation of cell lysates, cultured cells were washed with ice-cold PBS for 3 times, and an appropriate volume of RIPA lysis buffer was added to each well. Samples were kept on ice for minimum 30 min with occasional shaking and transferred to Eppendorf tubes subsequently. After centrifugation at 10,000 g for 10 min at 4 °C, the supernatant was collected and total protein concentrations were determined using Bradford assay. To quench the reaction, four-fifths of volume of 5× sample buffer was added into samples followed by heating at 95 °C for 5 min. The prepared samples were stored at -20 °C for further usage.

3.2.5.2 SDS-PAGE

Equal protein amounts of denatured samples were subjected to SDS-PAGE on 10% polyacrylamide gel. Electrophoresis was performed at 100 V for 20 min before the actual separation at 200 V for 45 min. The total protein amount of each lane was quantified using stain-free technology and molecular weight of the bands was assessed by comparison with a PageRuler Plus Prestained Protein Ladder.

3.2.5.3 Protein transfer and detection

The separated proteins were then transferred from the gel onto a PVDF membrane (0.45 μm pore size) using the electroblotting apparatus at 100 V for 90 min in the 4-degree room.

Then, the non-specific binding proteins were blocked with 5% Blotto-TBST for 2 h and the membrane was incubated in TBST containing primary antibody (1:1000) overnight at 4 °C with gentle agitation.

On the next day, the membrane was washed with 0.1% Tween-20 in TBST for 5 min 4 times, and following incubation with a suitable secondary HRP-conjugated antibody for 2 h at room temperature with gentle shaking.

To remove unbound secondary antibody, the membranes were washed with 0.1% Tween-20 in TBST for 4x 5 min each. And then incubation with HRP Homemade ECL solution shortly and expose the membrane by ChemiDoc Touch Imaging System to visualize the target proteins.

The detection of proteins was evaluated by measuring band intensities with ImageLab and normalized to the total protein amount (stainfree gel) as loading control.

Buffer and Solution	Component	Content
RIPA lysis buffer	NaCl	150mM
	1M Tris-HCl (pH 7.5)	50mM
	Nonidet P-40	1%
	Deoxycholat	0.25%
	SDS	0.1%
	H_2O	
5x sample buffer	3.125M Tris-Base	100 µl
	Glycerol	500 µl
	20% SDS	250 µl
	16% DTT	125 µl
	5% Pyronin Y	5 µl
	H_2O	20 µl
Separating gel	H_2O	9.15 ml
	30% PAA	7.5 ml
	Tris-HCl (pH 8.8)	5.625 ml
	TCE	225 µl
	10% SDS	225 µl
	TEMED	22.5 µl
	APS	112.5 µl

Stacking gel	H_2O	7.875 ml
	30% PAA	1.9125 ml
	Tris-HCl (pH 6.8)	1.125 ml
	10% SDS	112.5 µl
	TEMED	22.5 µl
	APS	112.5 µl
5x Electrophoresis buffer	Tris-Base	24.8mM
	Glycerol	191.8mM
	SDS	3.5mM
	H_2O	
5x Tank buffer	Tris-Base	25mM
	Glycine	192mM
	H_2O	
TBST (pH 8.0)	Tris-HCl	50mM
	NaCl	150mM
	Tween-20	0.1%
	H_2O	
Blocking solution	Tween-20	0.02%
	Non-fat dry milk/BSA	5%
	PBS	
HRP Homemade ECL	Luminal	1.25mM
	Cumaric acid	0.2mM
	1M Tris-Base (pH 8.5)	0.1mM
	30% H_2O_2	0.67%
	H_2O	

Table 3-7 Western blot buffers and solutions

3.2.6 Transfection

One day prior to the transfection, 450,000 cells/well were seeded in a 6 well plate. For each group, 1 µg of plasmid DNA was mixed with the Lipofectamine™ 3000 Reagent by using protocol from Thermo Fisher Scientific. Plate was incubated at 37 °C in a humidified incubator with 5% CO_2 for 24 h. Slug was knockdown by using DharmaFECT siRNA transfection protocol from Horizon. 300,000 cells/well cells were

seeded in a 12 well plate to be 70% - 90% confluent, a total amount of 5 µM SNAI2 (6591) siRNA was added to the DharmaFECT 1 Transfection Reagent complex and incubated for 24 h in incubator. The transfected cells were seeded in ibidi µ-Slide 8 well (45,000 cells/well) for further experiments.

3.2.7 Immunostaining and confocal microscopy

Cells in Ibitreat® 8 well µ-slides were washed with PBS+Ca^{2+}/Mg^{2+} and fixed with 4% formaldehyde for 15 min at room temperature. Fixed cells were rinsed with PBS for 10 min shaking and followed with different methods for distinct purposes.

3.2.7.1 Slug staining

Cells were permeabilized in 0.2% Triton-100 in PBS for 30 min and washed with PBS by 10 min shaking. After blocking with 1% BSA in PBS for another 30 min at RT, cells were incubated with slug primary antibody diluted in 0.2% BSA (1:200) overnight at 4 °C. Next day slide was then washed with 1% BSA in PBS for 3x 10 min and then incubated with secondary antibody (Alexa488, 1:400) and Hoechst 33342 (1:100) in PBS for 1 h. Finally, cells were washed for 2x 10 min with 1% BSA in PBS and once with PBS for 2x 10 min. Slides were sealed with FluorSave Reagent and stored at 4 °C in the dark.

3.2.7.2 Actin staining

Cells were stained with Hoechst 33342 and Rhodamin-Phalloidin for 1 h and then washed for 3 x 10 min with PBS at RT. Wells were sealed with FluorSave reagent and covered with 8 x 8 mm coverslips each.

3.2.7.3 Double staining

Cells were incubated in 0.2% Triton-100 in PBS for 30 min for membrane permeabilization. After 10 min washed with PBS, cells were incubated with 1% BSA

in PBS for 30 min with gentle shaking. Two primary antibodies were diluted in 0.2% BSA in PBS (1:200) and added 150 µl into each well. After overnight incubation at 4 °C, cells were washed with 3x 10 min with 1% BSA in PBS and then exposed to two different secondary antibodies (1:400) and Hoechst 33342 (1:100) in PBS for 1h shaking at RT. Finally, cells were washed for 2x 10 min with 1% BSA in PBS and once with PBS for 10 min. Slides were sealed with FluorSave Reagent, and samples were stored at 4 °C in the dark.

Cells stained only with secondary antibody were used as omission control to help identify non-specific binding of the secondary antibody or auto-fluorescence from the sample. Images were acquired with HC PL APO 40x/1.30 OIL or 63x/1.40 OIL immersion objective using the TCS SP8 SMD inverted confocal microscope. Scanning was performed with 400 Hz, and an average of four frames was acquired for the co-localization analysis channel in sequential mode. The following excitation laser lines were used: 405 nm, 488 nm, 552 nm and 638 nm.

Primary Antibody	Dilution	Species
Slug (C19G7)	1:200	Rabbit
Phospho-Histone H2A.X (Ser139)	1:200	Mouse
RPA32/RPA2 (ab2175)	1:200	Mouse

Table 3-8 Primary antibodies used for immunostaining

Secondary Antibody/Dye	Dilution	Species
Hoechst (bisBenzimide H 33342)	1:100	-
Rhodamine Phalloidin	1:400	-
Alexa Fluor 488	1:400	goat-anti-rabbit IgG
Alexa Fluor 546	1:400	goat-anti-rabbit IgG
Alexa Fluor 633	1:400	goat-anti-mouse IgG
Alexa Fluor 680	1:400	goat-anti-mouse IgG

Table 3-9 Secondary antibodies or marker dyes used for immunostaining

3.2.8 MTT assay

A stock solution of MTT was prepared by dissolving it in PBS to a concentration of 5 mg/ml. The number of 5,000 cells/well cells were seeded in a 96-well plate surrounded with PBS. Treatment was performed with indicated concentration and time in triplicates. Subsequently, 10 µl MTT stock solution were added to each well and incubated for 2 h at 37 °C in a humidified incubator. Subsequently, the culture medium was removed and 100 µl DMSO were added to each well to dissolve the formazan crystals. The plates were shake for 1 h and the absorbance was measured at 550 nm wavelength using TECAN reader.

3.2.9 Flow cytometry

Cells were seeded at a density of 5,000 cells/well in 12 well plates overnight and treated with the respective substances in triplicates. Harvested cells, medium and washing solution PBS were all transferred to flow cytometry tubes, and centrifuged with 600 xg for 10 min at 4°C. Debris or contaminants were washed with 1 ml PBS for two times centrifugation. Single-cell suspension exposed to a solution of propidium iodide (50 µg/ml) in PBS and immediately analyzed by flow cytometry for each measurement. Cells permeable for propidium iodide were considered as dead. For apoptosis measurement, the cells were resuspended in Nicoletti buffer (0.1% sodium citrate (w/v) + 0.1% Triton X-100 (v/v) in PBS), and incubated for 1 h, cells were collected by flow cytometry using BD FACS Canto II.

3.2.10 Pyrene polymerization assay

Pyrene actin 10% was dissolved with 1 ml ddH$_2$O to a final concentration of 1 mg/ml (24 µM), vortex gently and keep it on ice for 2 min. The pyrene actin buffer was transferred into a centrifuge tube and kept on ice for another 60min. Extract the supernatant after 60 min ultracentrifugation (55,000 rpm) at 4°C. F-actin buffer was

diluted with 0.5 ml ddH$_2$O first, and mixed with another 0.5 ml ddH$_2$O as a 10x stock solution. The final compositions were as follows:

Group	Reagent and Content
Baseline	30 µl ddH$_2$O, 5 µl F-actin buffer, 5 µl DMSO
Positive control	20 µl ddH$_2$O, 5 µl F-actin buffer, 10 µl MgCl$_2$ (10mM) and 5 µl DMSO
Compound	20 µl ddH$_2$O, 5 µl F-actin buffer, 10 µl MgCl$_2$ (10mM) and 5 µl compounds (dissolved in DMSO to 10mM)

Table 3-10 Reagents and contents for pyrene polymerization assay

The prepared mixed reagents were added into a 96-well half area black flat Bottom polystyrene NBS microplate before the rapid addition of 10 µl pyrene actin to start polymerization. Pyrene fluorescence was monitored every 20 s in a multimode plate reader at 360 nm excitation and 400 nm emission wavelength. Fluorescence intensity was recorded with 100 cycles for first generation compounds and 300 cycles for second generation compounds.

3.2.11 Proliferation assay

Hela cells were seeded at 3000 cells/well with triplicates for each condition. After 24 h, one plate was stained with 0.5% crystal violet for 10 min and washed with ddH$_2$O afterwards as baseline measurement. Selected compounds were prepared using DMSO (stored at -20 °C), and further diluted to the appropriate concentrations for the experiment. The cells in the proliferation plate were treated with gradient concentrations (200µM, 100µM, 30µM, 10µM, 3µM) of compounds for another 72 h, a total of 0.1% DMSO was set as the negative control group. The corresponding plates were stained and washed with the same procedure as baseline plate.

Trisodium citrate (7.35 g) was dissolved in 250 ml H$_2$O and further mixed with 250 ml 50% ethanol. The dried plates were redissolved in sodium citrate solution with 10 min shaking and measured with the microplate reader at an optimal wavelength of 550 nm. Three independent experiments were performed. For statistical analysis, the

mean value of control group was set to 100%, and the percentages of each group were normalized toward the control to quantify the effect on cell proliferation.

3.2.12 Scratch assay

Pre-coat the 96-well plates with PBS + Collagen G (0.5%) for 1 h at 37 °C. Hela cells (40,000 cells/well) were cultivated overnight until 90% confluence, the cell monolayer was scratched by an automatic scratcher with similar size in the middle of the well. Remove the debris by washing the plates twice with warm PBS+Ca^{2+}/Mg^{2+} and then replace with 100 µl complete medium with test compounds. Cells were treated with serial dilutions of the compounds in concentrations descending from 200 to 3 µM (the same as the proliferation condition). Control groups were treated with DMEM medium with 0.1% DMSO (baseline) or without FBS (positive). After 24 h for migration, the detached cells were washed with PBS+Ca^{2+}/Mg^{2+} once and dyed in addition to 0.5% crystal violet solution. Images were taken at 10x magnification using a standard inverted microscope. The wound area was calculated by ImageJ as the quantification of migration effects. Three independent experiments with triplicates were performed. For statistical analysis, the mean value of the control group was set to 100%, and the percentages of each group were normalized toward the control to quantify the effect on cell migration.

3.2.13 Statistical analysis

Three or more independent replicates were performed for each experiment. The protein level of western blot result was normalized with total protein and quantified by Image Lab™ Software. The data of MTT, flow cytometry, pyrene, proliferation and scratch assay were normalized to vehicle control (DMSO). All images of confocal imaging were evaluated using ImageJ version 1.53t. Data were presented as the mean values or mean ± standard error of the mean (SEM). Calculations of the half maximal inhibitory concentration (IC50), statistical analysis, and data plotting were

performed using Prism Version 9.5.1 (GraphPad Software, USA). Statistical methods and significances are indicated in the respective figures.

Potential synergism of combination treatment was assessed by calculation of Bliss value. Bliss values <0 were considered synergistic for MTT assay [71], and bliss values >0 were considered synergistic for Nicoletti assay [72].

Assay	Formula
MTT	Bliss value = $P_{combination} - P_{compound\ A}$ x $P_{compound\ B}$
Nicoletti	Bliss value = $P_{combination} - (P_{compound\ A} + P_{compound\ B} - P_{compound\ A}$ x $P_{compound\ B})$

Table 3-11 The formula of effect of drug combination as defined by Bliss Independence

Results - Part 1

The interaction of slug and actin in the DNA double-strand break repair

4. Results – Part 1

4.1 The interaction between slug and actin

4.1.1 Slug is a novel actin binding protein

Actin is regulated by interactions with various ABPs [73], the dynamics of actin influences many functions in the cells including migration [74], metastasis [75], apoptosis [76], DNA damage [77] and so on. Some potential ABPs (**Supplementary Table 8-1.1**) were screened out by using the Matchmaker Gold Y2H system, and the interactions between the proteins and actin were compared to the STRING database (https://string-db.org/). All screened out experiments were conducted and analyzed by Dr. Simone Moser (Prof. Vollmar, LMU Munich).

In this protein-protein interaction network (**Figure 4-1.1 A**), the predicted interactions of proteins are presented. The connected line between slug (SNAI2) and actin (ACTB) shows a text-mined interaction, suggesting an indeterminate but potential functional association of them [78]. As pointed out, slug was identified as an actin binding protein by Matchmaker Gold Y2H system. However, the predictive analysis based on STRING database was unable to provide sufficient evidence to support this association. Hence, the aim of this study is to verify the interaction between slug and actin, and to explore its function and mechanism.

Firstly, to further confirm the relationship between slug and actin in vitro, co-immunoprecipitation (Co-IP) experiments were carried out. Under control conditions, the bands detected from the IP samples demonstrated that slug could bind to actin (**Figure 4-1.1 B**).
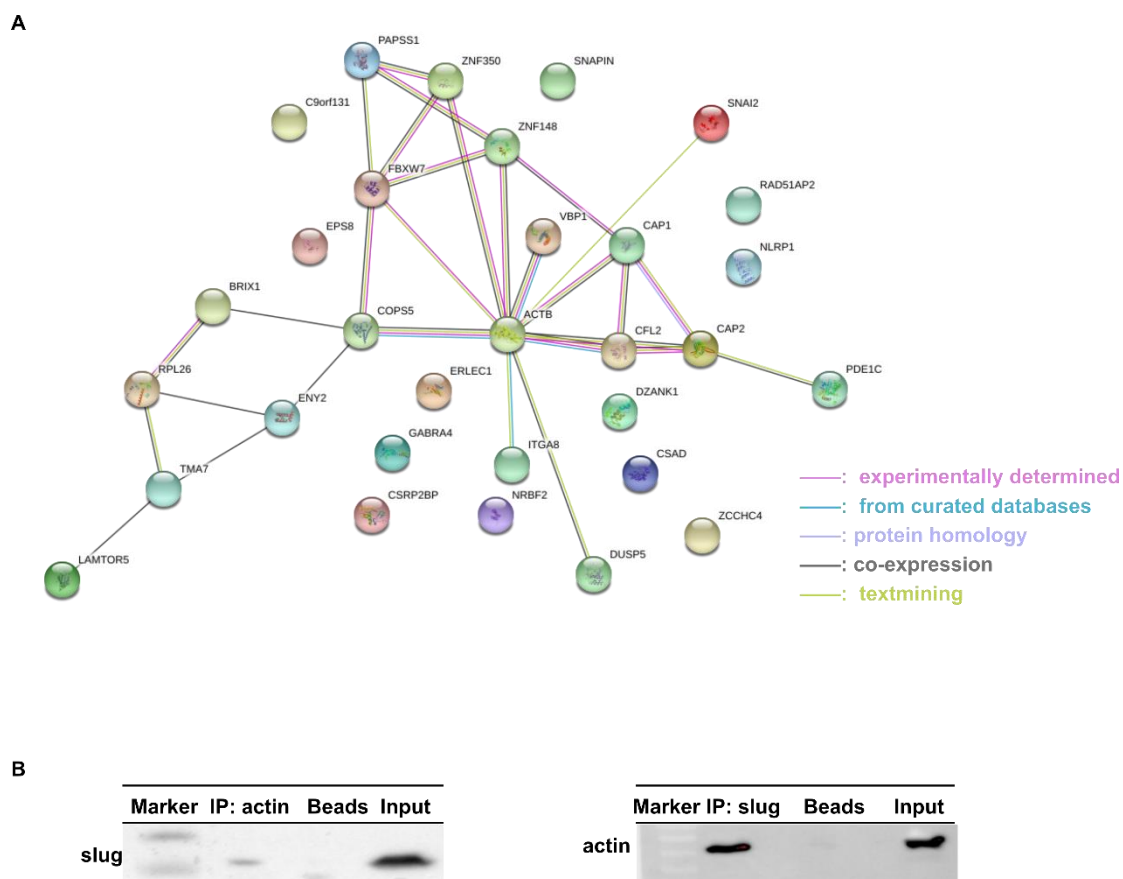
A

B

Figure 4-1.1 The validation of the interaction between slug and actin.

(A) String database network analysis of differentially expressed proteins identified by Y2H system. Lines with different colors represent the existence of different types of evidence applied to predict associations between actin (ACTB) and other proteins.

(B) Direct interaction between slug and actin in vitro. Co-IP of Hela cell extracts using either slug or anti-ACTB antibodies and blotted for anti-ACTB or slug protein, respectively. Proteins precipitated by microbeads in the absence of antibody served as a negative control. Purified total proteins were loaded as the input lane. (n=3)

4.1.2 Silencing of slug promotes aggregation of actin filaments

In view of the fact that ABPs play crucial roles in manipulating actin dynamics, including filament assembly [79], disassembly [80], cross-linking [81], and bundling [82]. We aimed to investigate, whether the regulation of slug expression could influence actin, thereby affecting the morphology of cells. Slug was knocked down using siRNA in Hela cells (**Supplementary Figure 8-1.2 A**), and Rhodamin-Phalloidin staining was performed to observe the cytoplasmic actin morphology. Compared with the control and non-targeting groups, silencing of slug resulted in the reorganization of cytoskeleton (**Figure 4-1.2 A**), the actin filaments tended to aggregate into the clusters. The extent of impact was quantified by counting the number of particles with ImageJ (**Figure 4-1.2 B**). In comparison to non-transfected control and the non-targeting group, the significantly increased number of particles in knockdown cells indicated that the slug depletion might cause F-actin polymerization.

Of note, overexpression of slug did not significantly affect the overall structure of the cytoskeleton. Slug was overexpressed by transfection of SlugMyc_pcDNA3 plasmid (**Supplementary Figure 8-1.2 B**), PBase plasmid was used as vehicle control since the treatment did not impact cell morphology under the chosen condition. Similar to non-transfected and the vehicle control, overexpressed cells still maintained a normal structure of the cytoskeleton (**Figure 4-1.2 C**), only a few cells showed some degree of damage, this might be due to the influence of lipofectamine™ 3000 reagents. Overexpression experiment was not quantified due to the software failure to identify particles in the images distinctly.

Summarizing, slug deficiency induced actin polymerization dramatically and led to aggregation of actin filaments. However, the overexpression of slug did not disrupt cytoskeleton morphology in Hela cells.
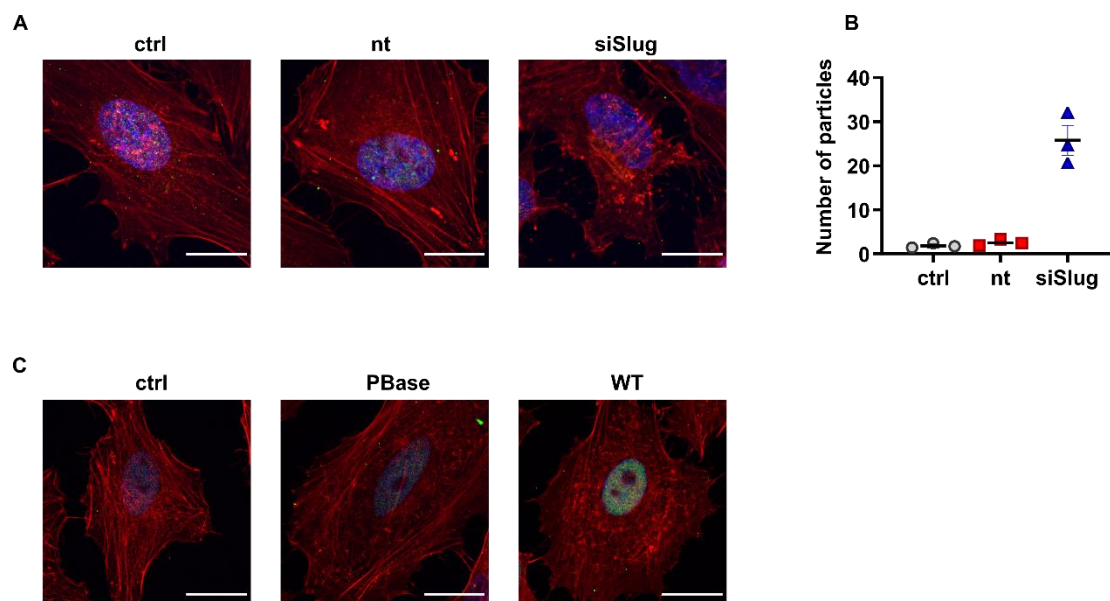
Figure 4-1.2 Effects of slug regulation on actin cytoskeleton.

(A) Silencing of slug gave rise to actin filaments aggregation. Slug was knocked down by using DharmaFECT 1 reagents to transfect siRNA in Hela cells, non-transfected and non-targeting groups served as controls. Actin morphology was visualized by Rhodamin-Phalloidin staining. (n=3, scale bar: 25 µm)

(B) The particles shown in the cytoskeleton increased significantly in silencing cells. The aggregation of F-actin was quantified by counting the particles number, 40 single cells were collected from duplicate wells. (n=3, mean ± SEM)

(C) Overexpression of slug did not affect cytoskeleton morphology. Cells were overexpressed with SlugMyc_pcDNA3 by using Lipofectamine™ 3000 reagents. Non-transfected and an empty vector PBase were served as controls. Actin morphology was visualized by Rhodamin-Phalloidin staining. (n=3, scale bar: 25µm)

4.1.3 Actin manipulation reduces slug levels in Hela cells

The association between slug and actin was further determined by using two well-known compounds for actin dynamics modulation, and the slug level was assessed after treatment. One substance in this study was latrunculin B (Lat B), a potent actin polymerization inhibitor, meaning that it disrupts the normal assembly of the actin cytoskeleton [83]. The other one was jasplakinolide (Jasp), its ability to promote actin polymerization leading to an accumulation of stabilized filaments within cells [84] (**Figure 4-1.3 A**).

At first, Hela cells were treated with 20nM and 100nM of the corresponding compounds for 24 h, slug protein levels were evaluated by Western blot. It was observed that the slug level was significantly decreased in jasplakinolide-treated cell as compared with that in DMSO-treated cells (**Figure4-1.3 B**).

Next, considering the human Slug protein (hSlug) is found in distinct foci within the nucleus [85], immunofluorescence staining experiments were performed after the same treatment to observe the slug intensity and localization in the nucleus. As shown in **Figure 4-1.3 C**, the decline of the nuclear-cytoplasmic (N/C) ratio in actin manipulation groups suggested that slug was diminished by actin binding compounds treatment.

Taken together, as a newly identified actin binding protein, slug levels in the nucleus were reduced by actin manipulation driven by Lat B and Jasp. Notably, when the cells were treated with 100nM Jasp, there was a significant reduction of slug levels compared to control cells.
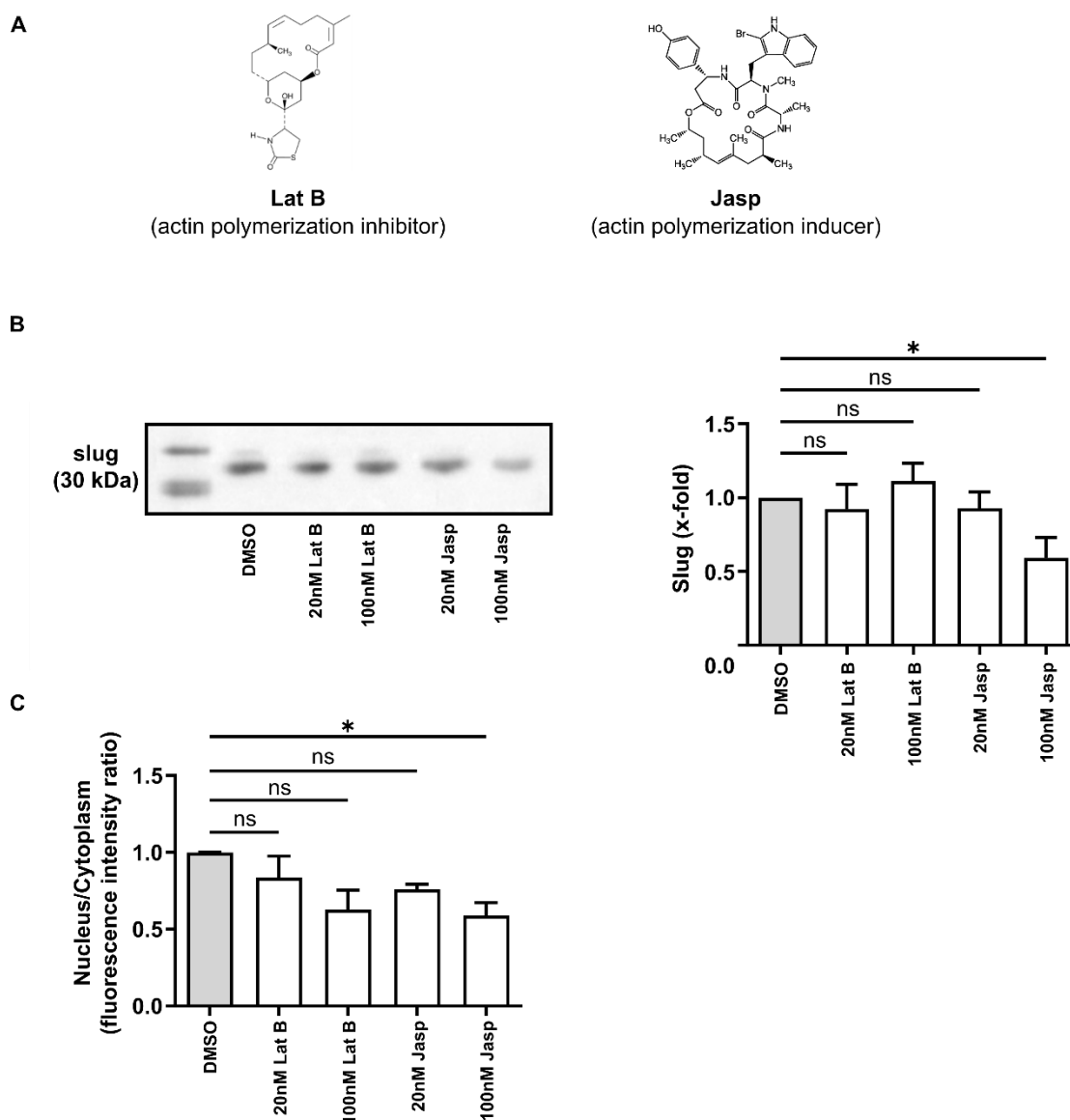
A

Lat B
(actin polymerization inhibitor)

Jasp
(actin polymerization inducer)

B

C

Figure 4-1.3 Manipulation of actin inhibits slug protein level in Hela and diminishes slug intensity in nucleus.

(A) The chemical structures of latrunculin B and jasplakinolide.

(B) Western blot analysis of the effect of actin binding compounds on slug protein level. Semi-quantitative analysis of the bands is shown. Protein level was normalized to vehicle control. Bar graphs revealed that 100nM Jasp induced a significant reduction of slug. (n=3, mean ± SEM, half-tailed unpaired equal-variance t-test, *P<0.05, ns: not significant)

(C) N/C ratio of slug after the addition of the indicated concentrations of Lat B and Jasp. The slug intensity in nucleus was diminished after 24 h treatment. The protein intensity was determined by confocal imaging. The N/C ratio were estimated by ImageJ software and normalized to vehicle control. (n=3, mean ± SEM, one-way ANOVA followed by Dunnett's multiple comparison test, *P<0.05, ns: not significant)

4.2 Combination of targeting actin with DNA damage for cancer therapy

One distinct role of actin binding proteins is co-localizing with DNA DSB sites and contributing to the repair process [43, 86]. When DNA damage exceeds the repair capacity of the cell or is severe enough to compromise cell viability, the cell may undergo apoptosis [87, 88]. However, the exact functions by which actin contributes to DDR and cell apoptosis are still being elucidated, and further research is needed to fully understand its role in these processes.

4.2.1 Combination with actin binding compounds is beneficial in doxorubicin induced apoptosis

Modern chemotherapy treatments use combinations of drugs simultaneously or sequentially to deal with the cancer [89]. Doxorubicin (doxo) is commonly used in the clinical therapy of cancers. It works by binding to the DNA and causing breaks in the double strands, which leads to the inhibition of cell division and eventually cell death [90, 91]. Regrettably, some side effects are caused consequently [92]. Thus, potential combination partners for doxo should be examined to accelerate cell death or to reduce the side effects.

To test if the combination of actin binders and doxo is synergistic, cells were treated with the indicated concentrations of Lat B or Jasp for 1 h before co-incubation with doxo for another 48 h. The apoptosis was determined by flow cytometry (**Figure 4-2.1 A**) and the cell death was measured by MTT assay (**Supplementary Figure 8-1.3 A**), both data were evaluated by using Bliss independence model (**Figure 4-2.1 B, Supplementary Figure 8-1.3 B**).

Individual treatment with doxorubicin in Hela cells only slightly affected apoptosis. Interestingly, the reduction of cell viability by additional application of actin substances showed synergistic effect in both assays. This dual-agent formulation implied that both cell death and apoptosis were increased with dose dependent manner when doxo treatment was combined with Lat B and Jasp.
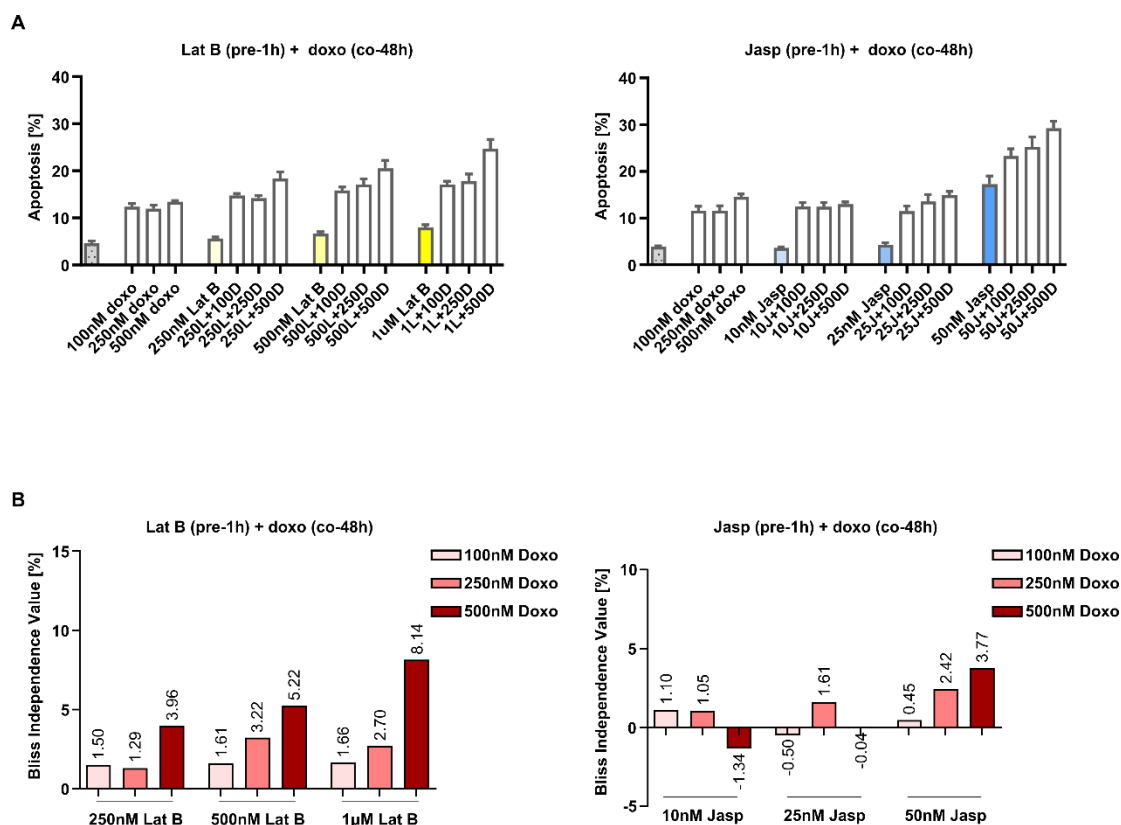

Figure 4-2.1 Effects of drug combination treatment on apoptosis induction in Hela cells.

(A) Actin binding compounds and doxo dose-dependently increased apoptosis in Hela. Cells were pre-treated with the indicated actin substances for 1 h and in combination with doxo, apoptosis was determined by flow cytometry after 48 h co-treatment. The percentage of apoptotic cells is shown. (n=3, mean ± SEM)

(B) Bliss independence analysis of apoptotic effect of dual-component model. Positive values represented synergistic potency. (n=3)

4.2.2 Latrunculin B promotes apoptosis in combination with UV exposure

Ultraviolet (UV) radiation can induce covalent bonds between adjacent pyrimidine bases in the DNA strand. These covalent bonds disrupt the normal structure of the DNA helix and can interfere with DNA replication and transcription processes and cause mutations and death [93-95]. As stated above, Lat B was identified as a positive candidate inducing apoptosis triggered by DNA damage. To further confirm the combination effects, Hela cells were pre-treated with 1μM Lat B for 1h, and DNA lesion was caused by 60 s UVA exposure subsequently. After 48 h incubation, the potency of the Lat B + UVA combination in Hela cells was tested by Nicoletti assay (**Figure 4-2.2 A**) and PI assay (**Supplementary Figure 8-1.4 A**), both data were assessed by using Bliss independence model (**Figure 4-2.2 B, Supplementary Figure 8-1.4 B**). The synergism between UV radiation and Lat B was demonstrated when compared to separate treatment.

Accordingly, the results implied a significant synergy of the conjugation of inhibiting actin polymerization and UVA-induced DNA damage, supporting the dose-effect analysis of apoptosis. These findings further emphasized that the therapeutic potential of combination of actin targeting compounds and the induction of DNA damage. Such combined synergistic potency could be highly beneficial for cancer therapy.
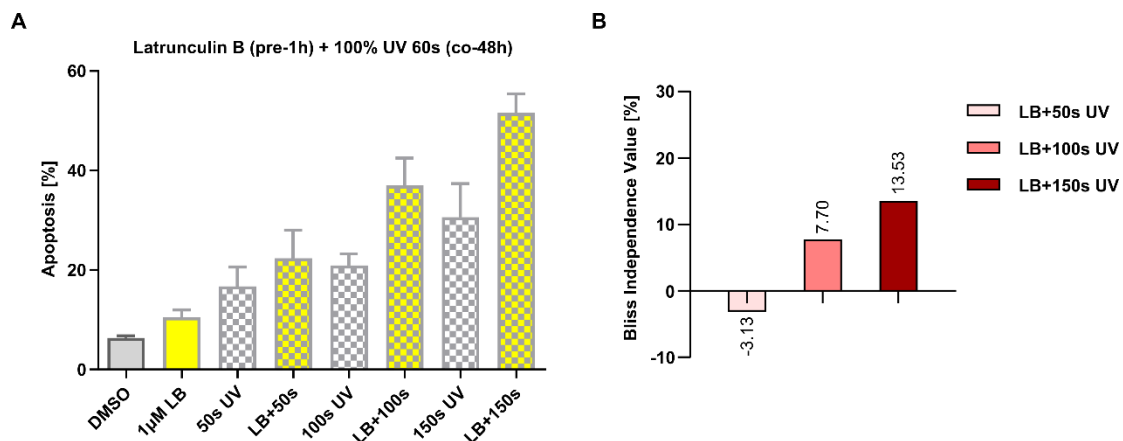
A

Latrunculin B (pre-1h) + 100% UV 60s (co-48h)

B

Figure 4-2.2 Apoptotic effect of Lat B-UVA model measured by flow cytometry.

(A) The combination of 1μM Lat B and UVA treatment acted synergistically. The apoptosis was determined by flow cytometry after 48 h. (n=3, mean ± SEM)

(B) Bliss independence analysis of apoptotic effects on the Lat B-UVA model. Positive values represented synergistic potency. (n=3)

4.3   The role of slug in doxorubicin induced DDR

The function of slug as a potential actin binding protein, remains to be elucidated. Based on the actions outlined above, targeting actin combined with DNA damage facilitate apoptosis. Herein, we focused the state of slug in doxo-induced DNA DSB repair. The design of this study was driven by the published hypothesis that slug has been implicated in the regulation of DNA damage response pathways [96, 97].

H2AX is a member of the core group of histones that contributes to nucleosome formation and DNA structure. When a DNA DSB is introduced into the genome, the H2AX histones near the break are phosphorylated by the ATM kinase at residue Ser-139. Upon phosphorylation H2AX is referred to as gamma-H2AX (γ-H2AX). Given that only H2AX histones near the site of DNA damage are phosphorylated, γ-H2AX is a useful target when determining the abundance and location of DSBs [98-101]. Precisely for this reason, the co-localization of slug and γ-H2AX was determined to decipher the correlation between slug and DNA DSB process.

In addition to γ-H2AX, Replication Protein A (RPA) is also important, which could bind to single-stranded DNA (ssDNA) and protects DNA ends from degradation [102, 103]. The human RPA (hsRPA) complex is composed of three subunits: RPA1 (17p13.3 RPA70), RPA2 (1p35 RPA32), and RPA3 (7p22 RPA14) [104, 105]. Among, RPA2 comprises multiple domains, including the DNA-binding domains, and their organization allows for efficient interaction with ssDNA [102, 106]. Furthermore, in consideration of the report that Jasp and Lat B could significantly inhibit the DNA repair leading to a marked formation of RPA-2 foci [107], the location of slug and RPA2 were validated simultaneously after doxo-induced DDR in this study.

Firstly, a DNA damage model was established by 250nM doxo treatment for 2 h, and then incubation with complete culture medium without doxo for DDR. Due to the different properties of γ-H2AX and RPA2, various time points were chosen for DDR.

Next, immunofluorescence double-staining experiments for slug/γ-H2AX or slug/RPA2 were performed to visualize the proteins in nuclei, as illustrated in the representative images. Finally, the intensity of the proteins was measured by ImageJ and the co-localization relationship between slug and the DNA damage factors were rated using the Pearson correlation coefficient [108].

The intensity of the three proteins were first increased and then decreased over time after DNA damage. The change of the proteins implied that all of them might relevant in cellular response to DNA damage (**Figure 4-3 A, B**). The Pearson values of slug and γ-H2AX remained around 0.17, indicating that less than 20% of slug site co-localized (weak positive) with γ-H2AX foci in this process. And, the results of slug and RPA2 ($\approx$0.33) revealed that slug co-localized with RPA2 site with a moderate positive linear relationship [109] (**Figure 4-3 C, D**). Briefly, the intensity of slug, γ-H2AX and RPA2 changed over time following dox-induced DDR. The co-localization analysis of slug/γ-H2AX and slug/RPA2 revealed not very strong but positive relationship in DSB repair process.
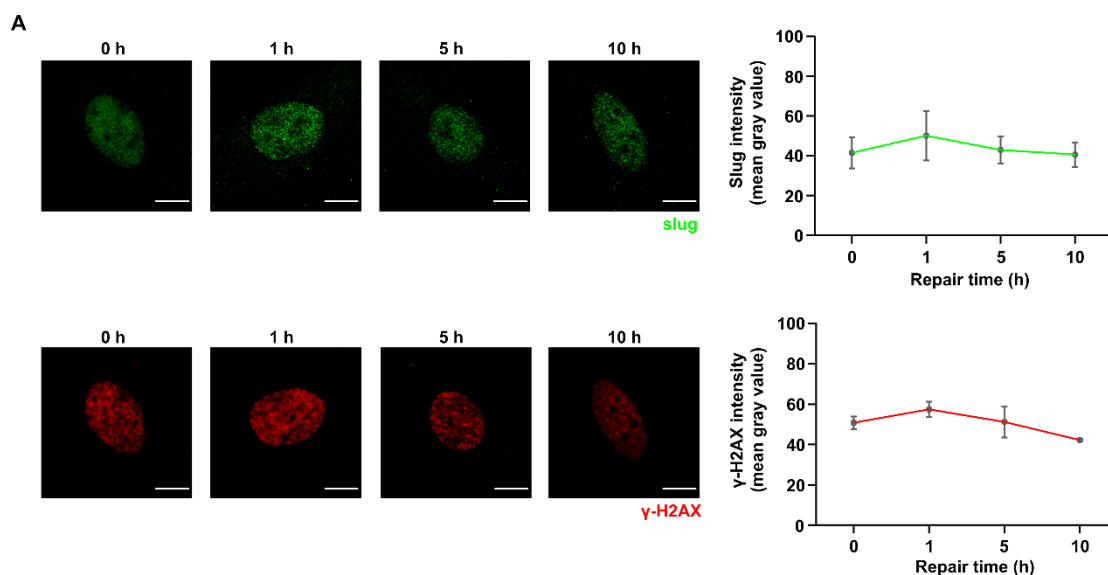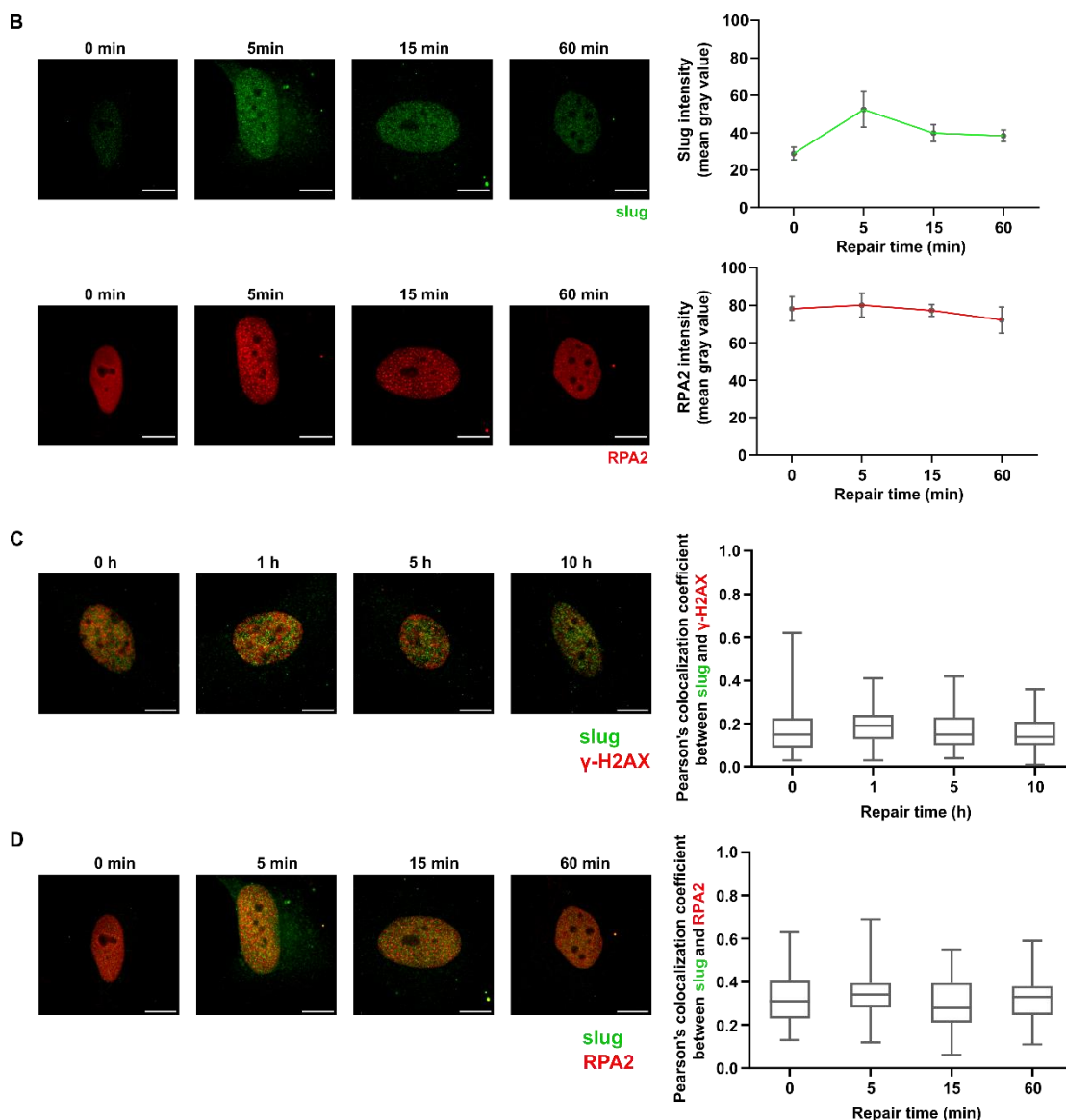
Figure 4-3 Slug as a potential target in doxo-induced DDR.

(A) The intensity of slug and γ-H2AX in DDR process.

(B) The intensity of slug and RPA2 in DDR process.

The quantification of intensity was evaluated by ImageJ with mean gray value.

(C) The co-localization of slug and γ-H2AX (r=0.17±0.01, P=0.091 [ns]).

(D) The co-localization of slug and RPA2 (r=0.33±0.01, P=0.244 [ns]).

The co-localization was classified using Pearson's colocalization coefficient values.

The following points are the accepted guidelines for interpreting the correlation coefficient: 0: no linear relationship, 0±0.3: weak positive (negative) relationship, ±0.3~±0.7: moderate positive (negative) relationship, ±0.7~±1: strong positive (negative) relationship, +1: perfect positive relationship, -1: perfect negative relationship. (n=3, mean ± SEM, scale bar: 10µm, single cell number for each group: 20, One-Way ANOVA followed by Kruskal-Wallis statistic, ns: not significant)

4.4 The relationship between slug and nuclear actin in DNA DSB repair process

4.4.1 Slug is bound to nuclear actin

Nuclear actin has been implicated in the regulation of the DNA repair pathway choice. It can interact with and modulate the activity of proteins involved in different DNA repair pathways to promote efficient and accurate repair [110-112]. Moreover, as noted above, slug was discovered as a novel ABP and as part of the DSB repair process. Therefore, we assumed that the participation of slug in the DNA damage response pathway might be connected to nuclear actin.

Hela cells were transfected with pmCherry-C1 actin-3XNLS P2A mCherry plasmid and Nuclear Actin-Chromobody plasmid (TagGFP2) to overexpress nuclear actin in different way (**Supplementary Figure 8-1.5**). The DNA DSB was activated by 250nM doxo for 2 h and subsequent DNA repair was proceeded with complete DMEM medium incubation for different periods (0 h, 1 h, 5 h). The Pearson correlation coefficient r value (0.3~0.4) showed that slug co-localized with nuclear actin during the DSB repair process. And the co-localization showed significant differences between repair groups from Nuclear Actin-Chromobody TagGFP2 overexpressed cells (**Figure 4-4.1 A, B**).
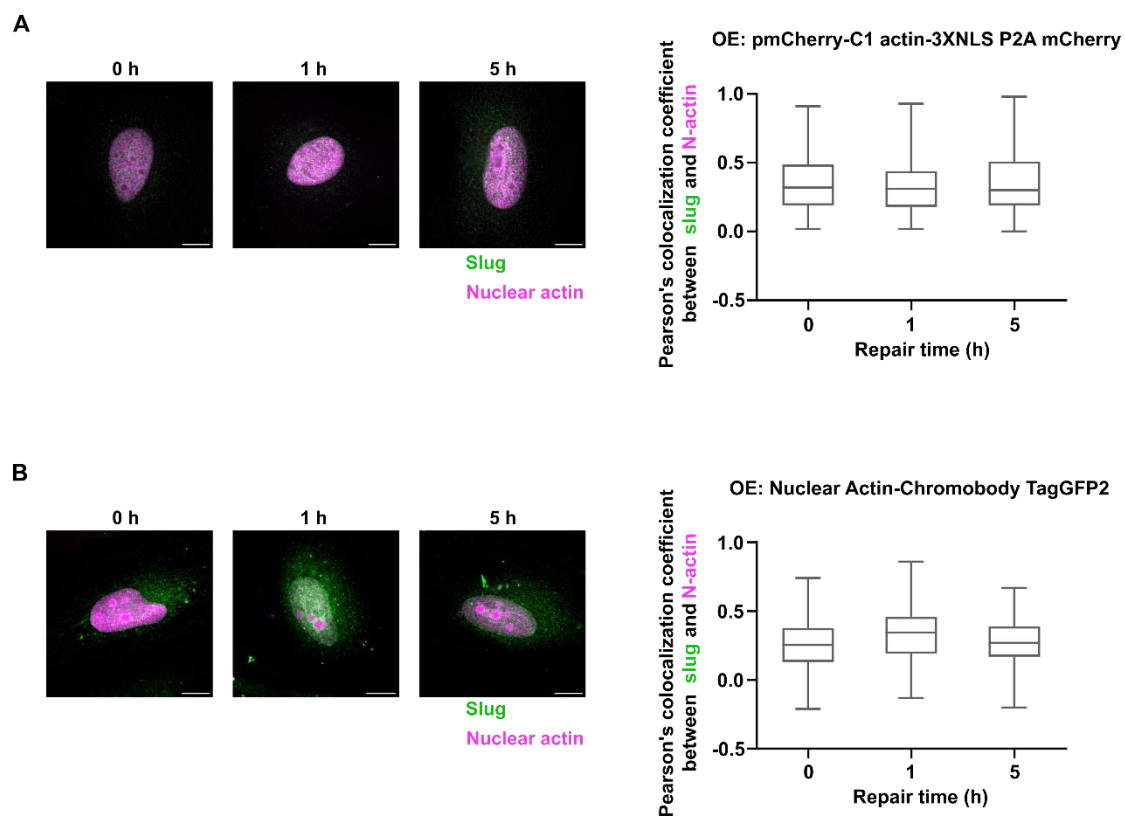
Figure 4-4.1 The co-localization between slug and nuclear actin in DDR process.

(A) The co-localization of slug and nuclear actin in pmCherry-C1 actin-3XNLS P2A mCherry plasmid overexpressed cells (r=0.35±0.03, P=0.625 [ns]).
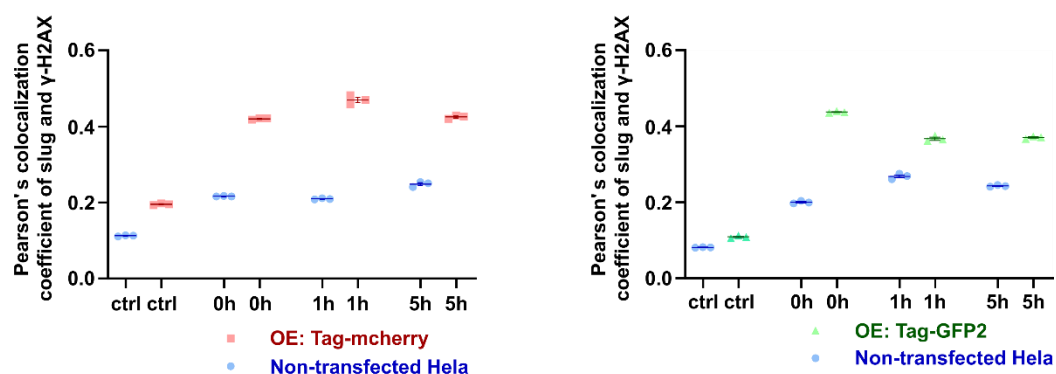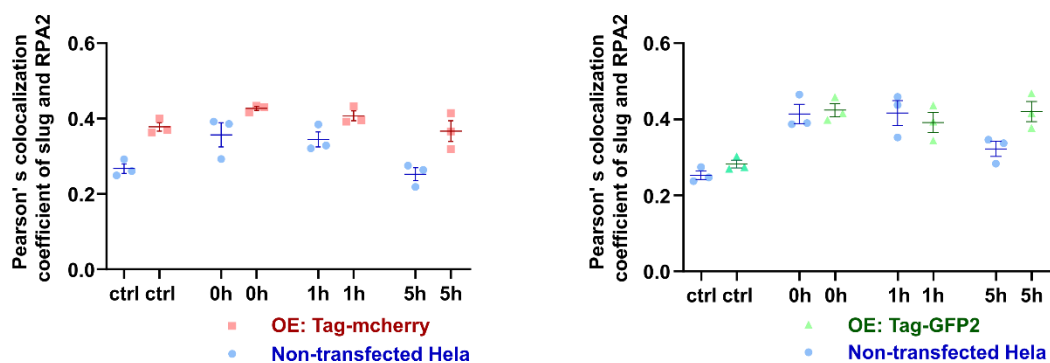
(B) The co-localization of slug and nuclear actin in Nuclear Actin-Chromobody TagGFP2 overexpressed cells (r=0.30±0.02, P=0.0003 [***]).

(n=3, mean ± SEM, scale bar: 10µm, single cell number for each group: 20, different square regions of each nuclear for evaluation:3, One-Way ANOVA followed by Kruskal-Wallis statistic, ***P < 0.001, ns: not significant)

4.4.2 The interaction of slug and nuclear actin might be involved in DNA DSB repair

To further explain the interaction of nuclear actin and slug in DNA damage in depth, nuclear actin was overexpressed with the same plasmids as above experiment. The DNA DSB was driven by 250nM doxo for 2 h, then the cells were cultivated without doxo for a period of time for damage repair. Finally, double staining was performed for assessing the co-localization of slug/γ-H2AX and slug/RPA2.

Surprisingly, the Pearson coefficient values of slug/γ-H2AX co-localization doubled and showed significant differences in repair process after the overexpression of nuclear actin (**Figure 4-4.2 A**). In contrast, there was no significant change of the r values of slug/RPA2 between non-transfected cells and overexpressed cells. However, it is worth mentioning that the co-localization of slug/RPA2 changed obviously during DSB repair (**Figure 4-4.2 B**).

A   **The co-localization of slug and γ-H2AX in nuclear actin overexpressed cells**

B   **The co-localization of slug and RPA2 in nuclear actin overexpressed cells**

Figure 4-4.2 Overexpression of nuclear actin influences the co-localization between slug and DNA damage factors.

(A) The co-localization of slug and γ-H2AX.

OE: pmCherry-C1 actin-3XNLS P2A mCherry (r=0.44±0.01, P=0.037[*]) vs ctrl: non-transfected Hela (r=0.22±0.01, P=0.923 [ns]);

OE: Nuclear Actin-Chromobody TagGFP2 (r=0.39±0.01, P=0.035 [*]) vs ctrl: non-transfected Hela (r=0.24±0.01, P=0.494 [ns]).

(B) The co-localization of slug and RPA2.

OE: pmCherry-C1 actin-3XNLS P2A mCherry (r=0.40±0.01, P=0.0034 [**]) vs ctrl: non-transfected Hela (r=0.32±0.02, P<0.0001 [***]);

OE: Nuclear Actin-Chromobody TagGFP2 (r=0.41±0.01, P=0.135 [ns]) vs ctrl: non-transfected Hela (r=0.38±0.02, P<0.0001 [***]).

The co-localization analysis ROI was n nucleus from slug channel. The co-localization was classified using Pearson coefficient values (n=3, mean ± SEM, single cell number for each group: 20, One-Way ANOVA followed by Kruskal-Wallis statistic, *P < 0.05, **P < 0.01, ***P < 0.001, ns: not significant).

Results - Part 2

Validation of AI designed potential actin binding compounds for drug discovery

5. Results – Part 2

5.1 Putative actin binding compounds predicted in silico were screened for effects on actin polymerization in vitro

The interaction of Kabiramide (KAB) related natural products and actin inhibit actin filament dynamics, the tris-oxazole macrolide structure of KAB plays a crucial role in inhibiting actin polymerization [113, 114]. In this study, KAB was used as a ligand to generate a set of binding sites. The convolutional layers of AtomNet® identified actin binding related features and then screened specific targets through remarkably large compound library. Lastly, predicted small molecules were synthesized and delivered to us to validate the capacity of polymerization inhibition of the potential actin binding compounds.

To test the predicted compounds in the regulation of actin dynamics, we initially investigated their influence on actin polymerization by using an in vitro pyrene assay. Three independent experiments with duplicates were performed for a first generation of 83 compounds. Seven compounds (compound1-7) were confirmed as inhibitors of actin polymerization (**Figure 5-1 A**). Based on the chemical structures of the selected compounds, a second generation of compounds designed for better cellular penetration was screened. One hit (compound8) was identified from 102 compounds by four independent repetitions with duplicates (**Figure 5-1 B**). The relative intensity of the actin polymerization reaction was lower in the presence of compound, illustrating the selected compounds inhibited actin polymerization.
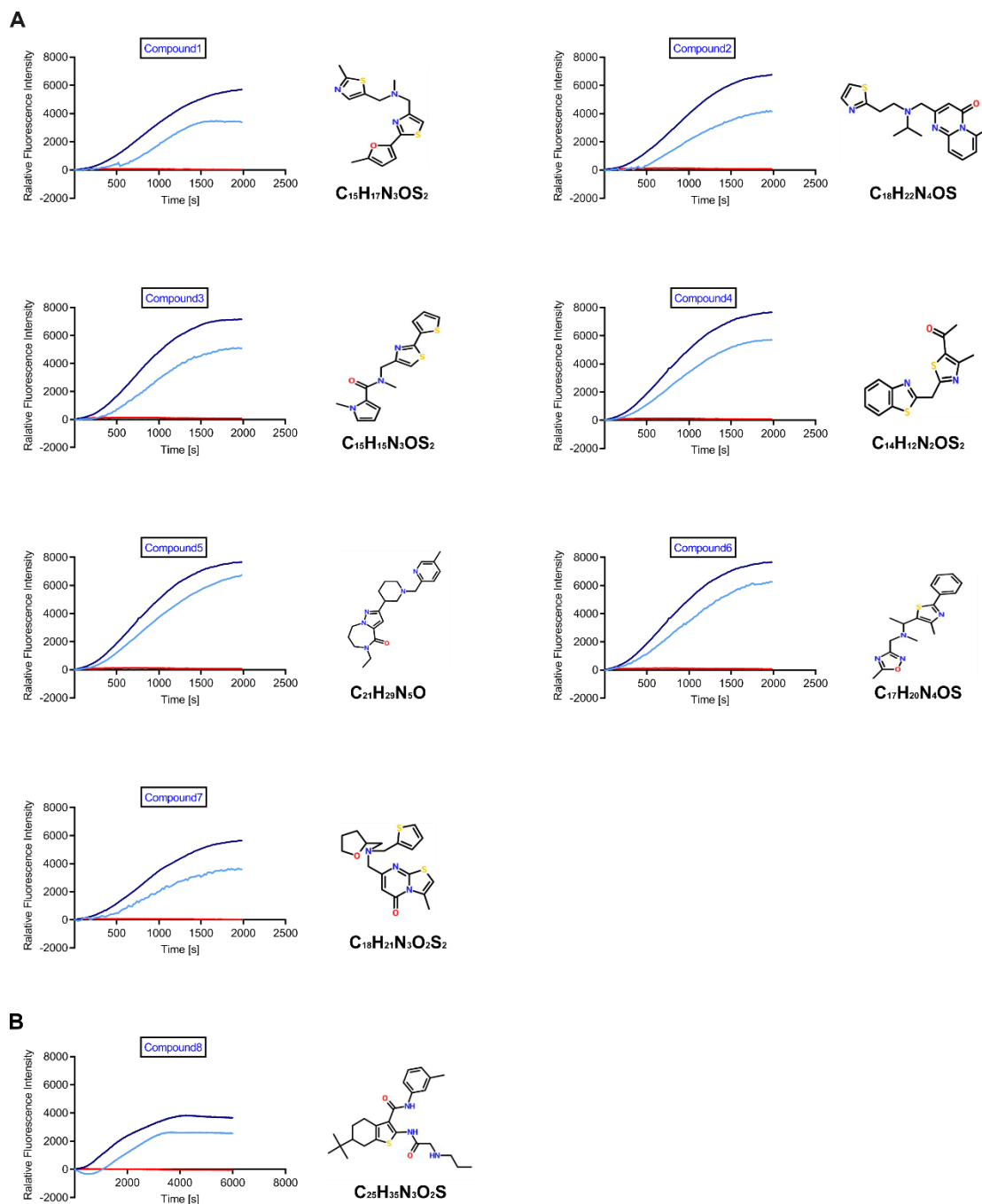
A

Compound1

$C_{15}H_{17}N_3OS_2$

Compound2

$C_{18}H_{22}N_4OS$

Compound3

$C_{15}H_{15}N_3OS_2$

Compound4

$C_{14}H_{12}N_2OS_2$

Compound5

$C_{21}H_{29}N_5O$

Compound6

$C_{17}H_{20}N_4OS$

Compound7

$C_{18}H_{21}N_3O_2S_2$

B

Compound8

$C_{25}H_{35}N_3O_2S$

Figure 5-1 Eight compounds were screened out as putative actin binding inhibitors.
(A) Seven compounds were selected from 83 candidates of the first generation. The actin polymerization was inhibited by the compounds. The chemical structures and formulas were provided by Atomwise using mcule. (n=3, 100 cycles)
(B) One compound was selected from 102 candidates of the second generation. The actin polymerization was inhibited by compound8. (n=4, 300 cycles)

Fluorescence intensity in normalized units is plotted versus time as an indicator for actin polymerization. Data were normalized to the initial value (time=0s) and presented as mean values. ——: base line, ——: positive control, ——: compound sample.

5.2 The selected compounds showed inhibition of cell proliferation

The eight compounds were dissolved with sterile DMSO to a 200mM stock solution. Because compound7 and compound8 caused solubility issues, they were excluded from further cellular testing. To examine the global effect of the six compounds, Hela cells were treated with these compounds at concentrations of 3, 10, 30, 100, 200µM in 96-well plates. Fluorescence was measured after 72 h treatment by crystal violet staining.

Proliferation was inhibited in a dose-dependent manner and was markedly reduced at higher concentration treatment (**Figure 5-2 A**). Especially, 200µM of compound2, compound3, compound4 and compound5 led to more than 50% of the extent of proliferation. Half maximal inhibitory concentration (IC50) parameters were used to evaluate compound potency (**Figure 5-2 B**). The calculated values for Hela cells were approximately 100µM to 200µM, respectively. Together, these data supported the high concentration compounds treated cells displayed a defect in proliferation.
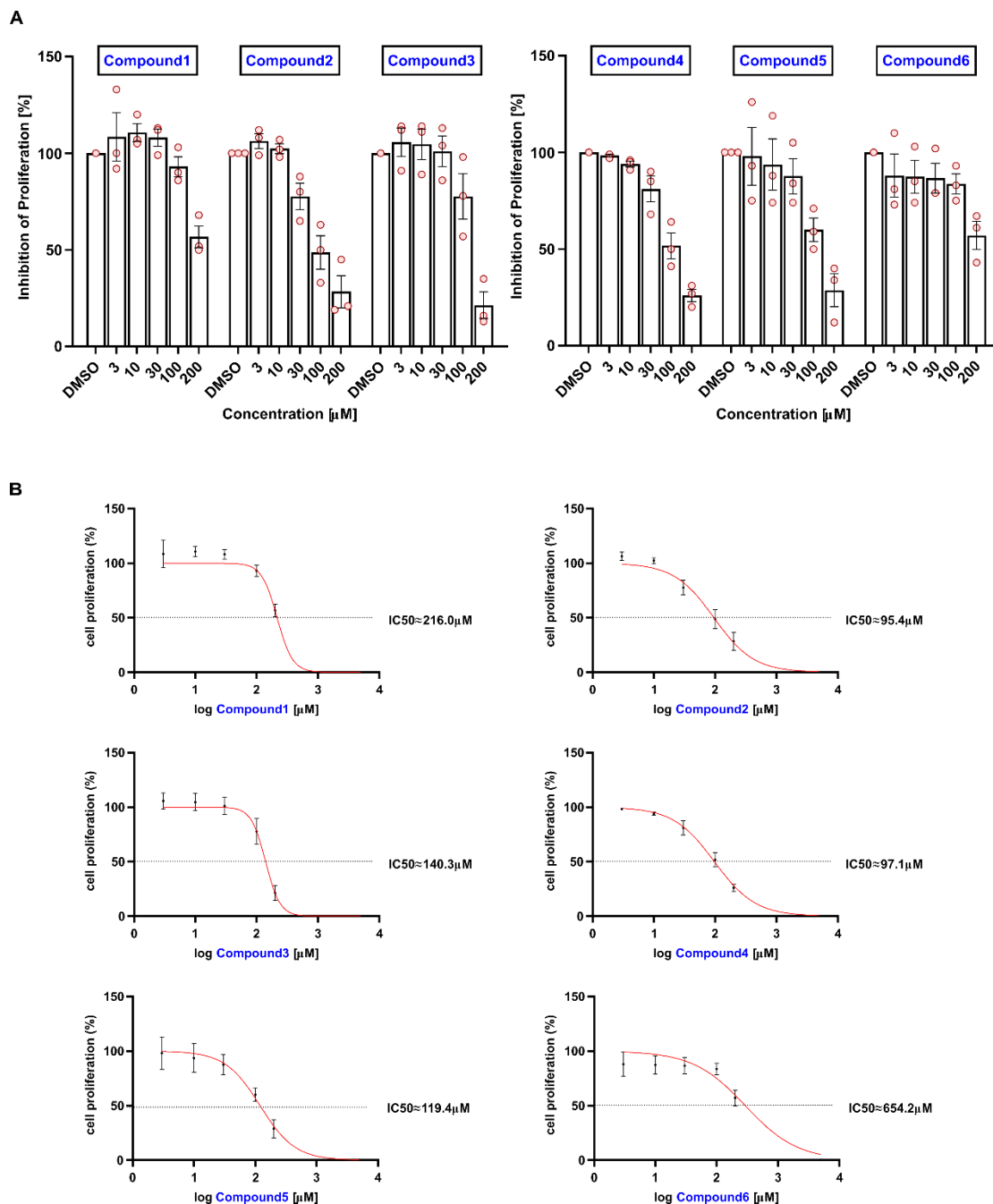
Figure 5-2 The proliferation of DMSO- and compound-treated Hela cells.
(A) The adsorption of crystal violet was quantified. The values obtained from treated cells at 72 h were normalized to the 0.1%DMSO control sample. (n=3, triplicates, mean ± SEM)
(B) Half inhibitory concentration (IC50) values for proliferation were calculated for each compound from the results in panel A. The dashed lines indicated a 50% reduction in cell proliferation. (n=3, mean ± SEM)

5.3 The selected compounds inhibited cell migration

Since actin cytoskeleton plays a crucial role in cell migration, we assessed the effects of the compounds on cellular motility in a scratch assay. Migration was suppressed by the compounds at high concentration (**Figure 5-3 A**). By contrast, 200µM of compound4 and compound5 exerted a higher inhibitory effect on the migration, showing more than 50% unhealed area. The wound area variation of different compounds was shown in **Figure 5-3 B**.
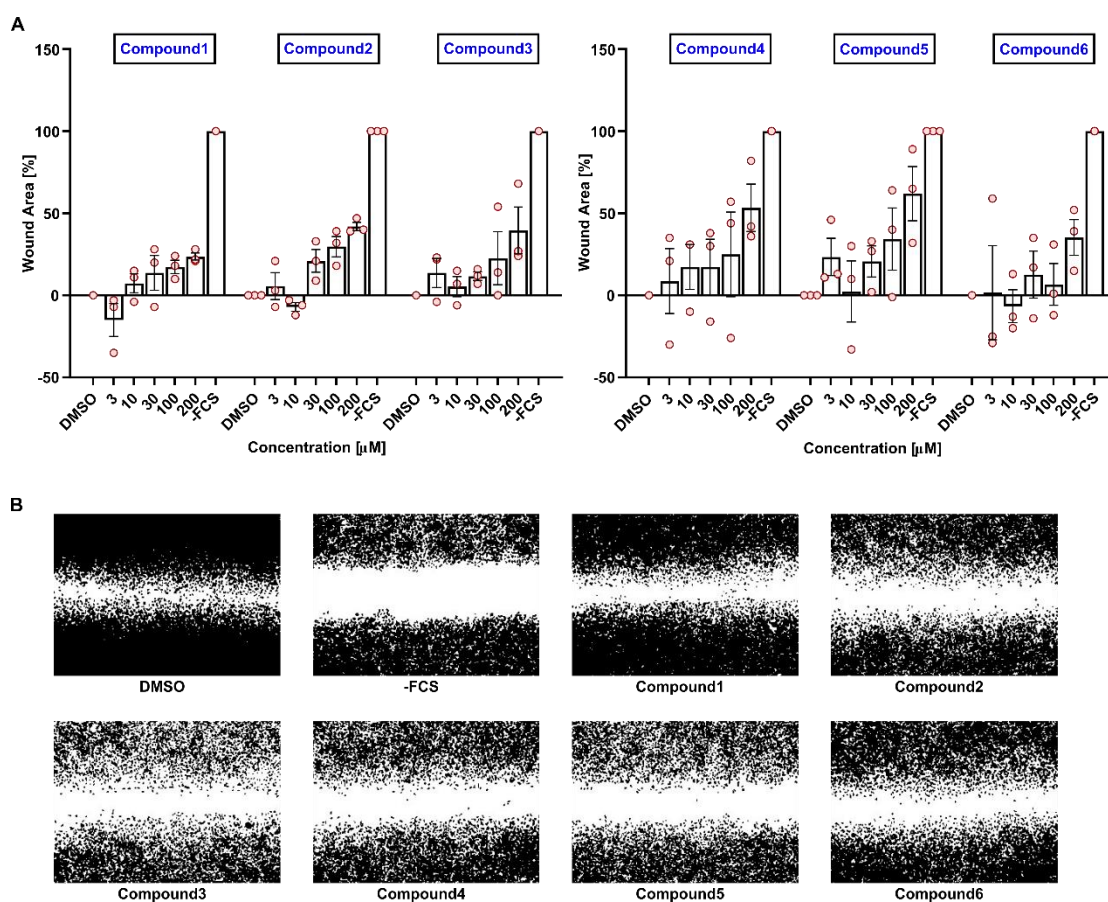

Figure 5-3 Scratch assay analyzing the effects on the migration of Hela cells.
(A) Relative migration was measured by quantifying the width of the wounds. The 0.1% DMSO was set as the baseline, and -FCS indicated cells incubated with DMEM medium without FCS as a positive control (100%, no migration), the values of the compound group were normalized to -FCS group (n=3, triplicates, mean ± SEM).
(B) Images were acquired at 24 h in vitro scratch assay. Representative images of scratched and recovering wounded areas on confluence monolayers of Hela cells with treatment.

5.4 The selected compounds changed the morphology of the actin cytoskeleton

The influences of selected compounds on actin cytoskeleton were further studied. The surviving cells after 24 h treatment with slightly different morphology as shown in F-actin staining images (**Figure 5-4**). As a positive control of polymerization inhibitor, 500nM Lat B accelerated F-actin disassembly. And actin was notably missing from actin skeleton regions in another positive control treated with 100nM Jasp. Actin was also reduced in cells treated with 200µM of selected compounds in varying degrees but had no obvious effect on the global distribution of F-actin networks. Interestingly, compound2 and compound5 induced actin skeleton aggregation with losing their initial spindle shape.
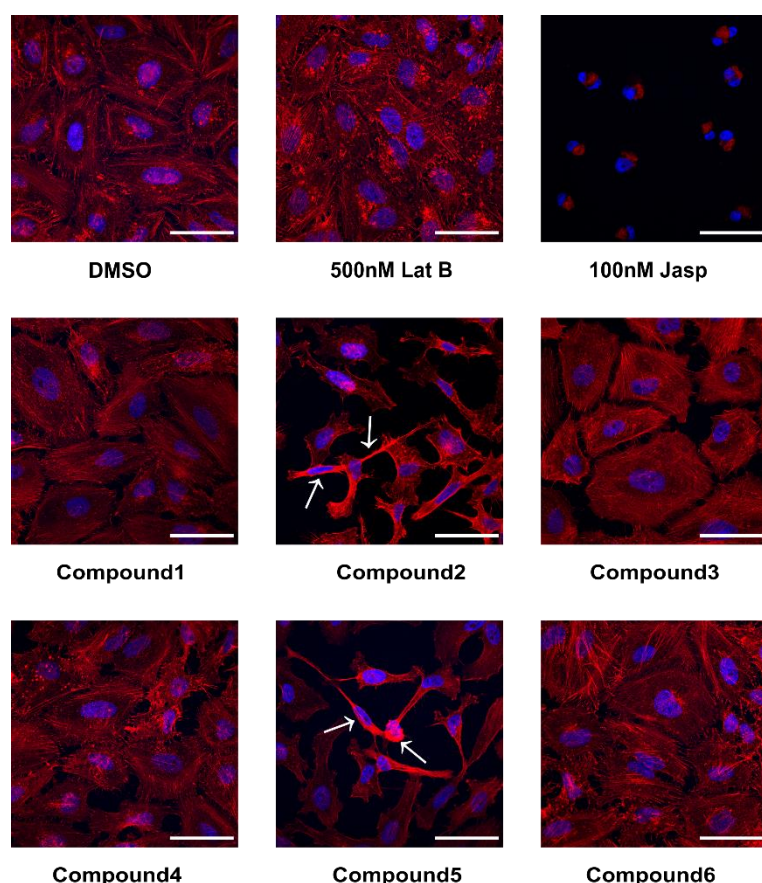

Figure 5-4 Actin morphology of Hela cells stimulated with the indicated concentrations of compounds for 24 h.
Representative microscopic images of Hoechst 33342 (blue) staining for nuclei and rhodamine-phalloidin (red) staining for F-actin. (n=3, duplicates, scale bar: 50µm)

Discussion

6. Discussion

6.1 Part-1

6.1.1 Slug is a novel actin binding protein

Actin binding proteins (ABPs) play crucial roles in regulating the organization and dynamics of actin filaments, which are essential for various cellular processes including cell motility, shape maintenance, and intracellular trafficking. Dysregulation of ABPs has been implicated in cancer progression and metastasis [115]. Therefore, targeting ABPs has emerged as a potential strategy in cancer therapy.

The yeast two-hybrid (Y2H) system is a molecular biology technique used to study protein-protein interactions in living cells. It is a powerful tool for identifying and characterizing protein interactions by screening large libraries of proteins for interacting partners and has been widely used in basic research [116]. The principle behind the Y2H system is based on the modular nature of transcription factors. In this system, two proteins of interest are fused to different components of a transcription factor, typically a DNA binding domain (BD) and an activation domain (AD). If the two proteins interact, the BD and AD will be brought into close proximity, allowing the transcriptional activation of reporter genes that are under the control of specific DNA sequences and leading to growth on selective media or expression of a reporter protein [117, 118].

In this study, some potential ABPs were screened out by Y2H system, some of them have previously been reported to be associated with actin. For example, cyclase-associated protein 2 (CAP2) can regulate the availability of G-actin for polymerization and control the rate of actin filament growth. In addition to its role in actin dynamics, CAP2 has been implicated in various cellular processes such as endocytosis, vesicle trafficking, and cell motility. Its precise mechanisms of action and its involvement in cancer biology are still being investigated [119, 120].

Although Y2H can be used to study protein interactions in their native cellular environment, as yeast is a eukaryotic organism, it is important to note that interactions identified using this system need to be further validated using additional techniques. Thus, in order to confirm the relationship between these proteins and actin, the predicted proteins were fed into the STRING database. STRING is a comprehensive online resource that provides information on protein-protein interactions (PPIs) and functional associations among genes and proteins. It consolidates data from various sources, including experimental studies, computational predictions, and publicly available databases, to construct protein interaction networks. These networks provide insights into the physical and functional associations among proteins [78]. On the basis of the network result, slug was suggested to be a novel actin binding protein. Further, two contrary Co-IP experiments were also used to validate the interaction between slug and actin in Hela cells.

Taken together, the slug was screened out as a potential actin binding protein by the Y2H system. However, the scant experimental evidence in the STRING database suggested that it may be a novel interaction. Notably, our Co-IP verification strongly supported that slug could bind with actin in Hela cells.

6.1.2 The interaction between slug and actin

Actin filaments are key components of the cytoskeleton and play essential roles in cellular processes [121]. Regulation of actin filament dynamics is a complex and important process in cell biology, and some commercial actin binding compounds are used for specifically manipulate this dynamic process [122]. One of these compounds is latrunculin B (Lat B), which binds to actin monomers and prevents their polymerization into actin filaments [123]. The other compound, Jasplakinolide (Jasp), that stabilizes actin filaments, promoting actin polymerization in vitro by stimulating actin filament nucleation [124]. Analysis of Western blot results revealed that high

concentration of Jasp might inhibit the expression level of slug protein. Meanwhile, the N/C ratio of confocal imaging illustrated that the actin polymerization dynamics might reduce slug level in the nucleus.

The use of siRNA to knock down slug expression has been applied to study the importance of slug in regulating cell morphology, EMT marker expression, and functional consequences [125, 126]. And, overexpression of slug in malignancy using the single-plasmid system has revealed a specific function for slug in the pathogenesis of mesenchymal tumors [127]. Here, we found that silencing of slug induced actin filaments aggregation in Hela cells, suggesting if the slug is knocked down, it may result in the loss of actin. This disruption can lead to the disassembly or reorganization of the complexes and potentially impact actin dynamics itself, further affecting cell function. However, no significant influence of slug overexpression on actin was found.

In short, proteins interact with each other through specific binding sites, manipulating one of the proteins can cause functional impacts on the other one. Our findings indicated that the binding of slug and actin could be regulated by actin dynamics, and depletion of slug promoted actin polymerization in the cytoskeleton. This strengthens the hypothesis on the interaction of slug and actin on a functional level.

6.1.3 Combination targeting actin and DNA damage is a promising model for cancer therapy

Combination therapy is an approach to cancer treatment that involves using multiple treatment modalities simultaneously or sequentially to enhance the effectiveness and to improve patient outcomes. These modalities include surgery, radiation therapy, chemotherapy, immunotherapy and targeted therapy. The goal of combination therapy is to exploit different mechanisms of action and attack cancer cells through

multiple pathways, increasing the chances of tumor regression and reducing the likelihood of resistance development [128-130]. Therefore, the implementation of combination therapy holds important clinical value.

Cancer is a complex disease that often involves multiple molecular pathways. By combining treatments that target different pathways, combiantion therapy can effectively disrupt cancer cell growth and survival. In detail, clinical trials have demonstrated the effectiveness of the doxorubicin (doxo) and paclitaxel (PTX) combination in treating metastatic breast cancer. Doxo, an anthracycline, works by inhibiting DNA replication and damaging cancer cells, while PTX, a taxane, disrupts cell division by stabilizing microtubules. By combining these two drugs, the treatment can target cancer cells through multiple pathways and increase the overall response rate [131]. Similarly, we tested the apoptosis of Hela cells with the combination doxo and actin binding compounds. In comparison to monotherapy, this treatment showed synergistic effects on apoptosis. In this context, we assumed that both Lat B and Jasp are effective options to combination chemotherapy with doxo.

Similarly, different treatment modalities can also have complementary effects when used together. For example, combining chemotherapy drugs with radiation therapy can enhance the killing of cancer cells by increasing DNA damage or impairing repair mechanisms. For instance, demethoxycurcumin (DMC) in combination with ultraviolet radiation B (UVB) has been shown to induce apoptosis, or programmed cell death, through the mitochondrial pathway and caspase activation in A431 and HaCaT cells [132]. In the same manner, we measured the apoptotic rates in a Lat B and UVA combination model, and the increased apoptosis provided the beneficial experimental basis for studying clinical cancer therapy and the exact underlying mechanisms.

In summary, these results demonstrated that targeting actin showed synergistic effects on apoptosis in combination with doxo or UV exposure.

6.1.4 The interaction of slug and actin in DNA DSB repair

DNA damage refers to any alteration or modification in the structure of DNA molecules, such as breaks, mutations, or chemical modifications. Several factors can cause DNA damage, including exposure to environmental toxins, radiation, certain chemicals, and even normal cellular processes. When DNA damage occurs, the DNA repair machinery is activated to fix the damage. However, if the damage is severe or the repair mechanisms are impaired, the DNA damage can persist. This persistent DNA damage can lead to genetic mutations, genomic instability, and ultimately contribute to the development of cancer [133-135]. Cancer cells often exhibit increased DNA damage and impaired DNA repair mechanisms, making them more susceptible to genetic abnormalities and further genomic instability [136].

Doxorubicin (doxo) works by interfering with the growth and replication of cancer cells. It does this by inhibiting the action of topoisomerase II, an enzyme involved in DNA replication and repair. By binding to DNA, doxo can induce breaks in both strands of the DNA double helix. Double-strand breaks (DSBs) are highly detrimental to cells because they can lead to chromosomal rearrangements and loss of genetic material, this helps to prevent cancer cells from dividing and multiplying. Despite extensive clinical utilization, it can also cause several side effects including nausea and vomiting, hair loss, increased risk of infection and potential damage to the heart in some cases [92]. Thus, exploring the mechanism of doxo-induced DSBs can help improve its first-line therapy.

Functions for nuclear actin in DNA damage are slowly beginning to emerge. Nuclear actin polymerization regulated by ARPs promotes DSB dynamics [111], and the co-localization of actin and RPA32 reveals that nuclear actin is recruited to sites of HDR [43]. Similarly, the involvement of slug in the activation of RPA32 suggests its potential importance in facilitating HR-mediated DSB repair [137], and the recruitment of RPA2 also relies on actin [107]. Moreover, the loss of nuclear actin

leads to the accumulation of DSB foci [138], and slug-depleted cells exhibit persistent γ-H2AX foci and failed recruitment of RPA [54]. These studies demonstrate that both nuclear actin and slug are required for efficient DSB repair. However, their interaction in DSB repair has not been elucidated.

Herein, doxo induced DSB was chosen as a capable model to study the implication of slug and nuclear actin interaction in DDR. Firstly, the slug was shown to be involved in DSB repair process. This finding was drawn from the change of the slug intensity in the nucleus. Secondly, we expressed nuclear actin tagged with an NLS and fluorescent proteins, the co-localization of slug and nuclear actin showed significant differences in the DSB repair assessed using Pearson coefficient values. This strongly supported the joint roles of slug and nuclear actin in this process. Last but not least, the co-localization coefficients of slug and DSB factors increased in actin-overexpressed cells. And the significant differences changed in the repair process when compared to non-transfected cells. This indicated that the recruitment of the slug at damage sites is increased when more nuclear actin is expressed. In other words, the enriched nuclear actin might contribute to slug recruitment to DSB foci and further facilitate the DSB repair process.

6.1.5 Conclusion and outlook

In this work, slug is identified as a novel actin binding protein, and the silencing of slug is shown to induce actin filament polymerization. On the other side, manipulation of actin dynamics synergistically increases the apoptosis of Hela cells. Furthermore, slug and nuclear actin interact during DSB repair. Overexpression of nuclear actin promotes slug to colocalize with γ-H2AX and RPA2 foci, which sheds light on the mechanism of the requirement of slug and actin in DSB repair and the function of the interaction between slug and nuclear actin in DDR process (**Figure 6**).
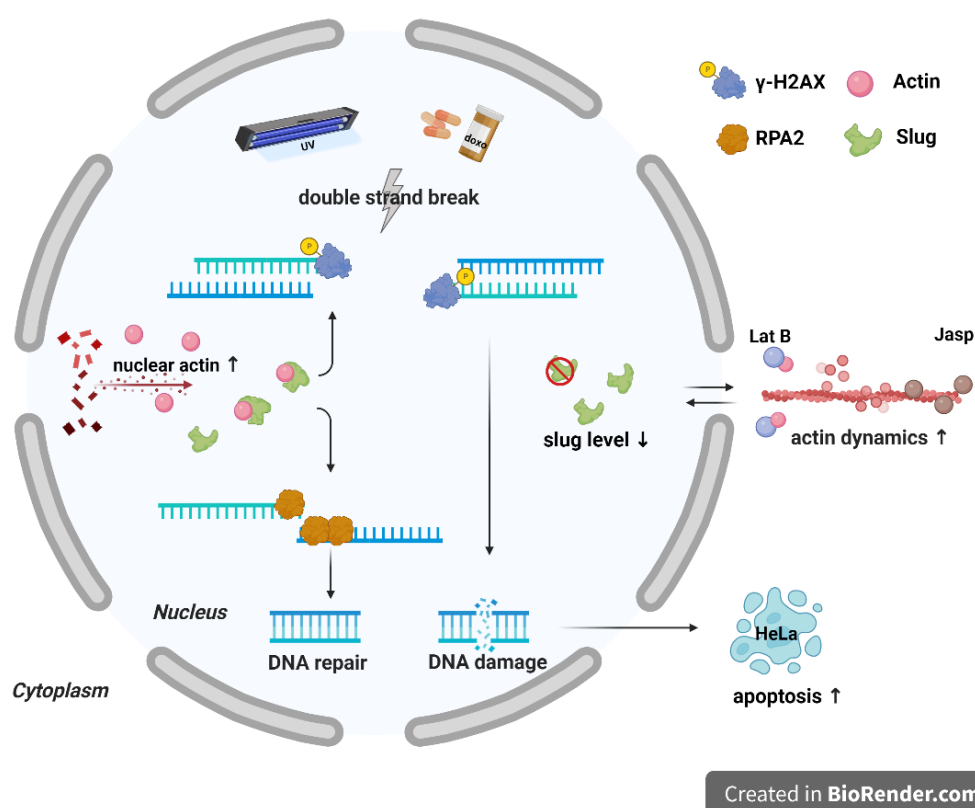

Figure 6 The interaction of slug and actin in the DNA double-strand break repair.

For further investigation, DSB should be induced in different way like Ultraviolet (UV) radiation. UV is classified into three main types based on the wavelength: UVA (longest wavelength), UVB, and UVC (shortest wavelength). Of these, UVB radiation is the most potent in terms of causing DNA damage, including DSBs. UVB radiation has enough energy to directly interact with DNA molecules and cause chemical alterations. These DNA lesions, such as CPDs and 6-4 photoproducts, distort the

DNA helix and interfere with DNA replication and transcription [94, 139]. Due to complicated mechanism of DNA damage induction by doxo, it is worthwhile trying to induce DSB by UV exposure to improve this project to the next level.

Moreover, in eukaryotic cells, actin is present in both the cytoplasm and the nucleus. To maintain the balance between cytoplasmic and nuclear actin, cells employ an export-import system. Inside the nucleus, actin interacts with actin binding proteins and participates in nuclear processes. Conversely, the export of actin from the nucleus to the cytoplasm is mediated by exportins [140]. By studying the complete set of proteins in a biological system, proteomics is an essential tool in deciphering the functional relationships, signaling pathways, and regulatory mechanisms underlying biological processes. The function and mechanism of the interaction between slug and actin can be also explored by proteomics in the future.

6.2 Part-2

6.2.1 Development and screening of putative actin binding compounds

Combining in silico methods with biomedical experiments is a powerful approach to accelerate drug design and development [141]. Atomwise is a biotechnology company that specializes in using artificial intelligence (AI) and machine learning for drug discovery. Their key offering is its AtomNet® platform, which utilizes deep learning algorithms to predict the binding affinity between small molecules and target proteins. By analyzing billions of data and leveraging its AI models, Atomwise can rapidly screen and identify potential drug candidates for a wide range of diseases [68]. However, the final validation and development of these small molecules and target proteins still require rigorous in-lab experiments and clinical trials.

Based on the AtomNet® technology, a natural compound Kabiramide (KAB) was used as a ligand to develop a batch of small molecules. Seven compounds were validated as actin polymerization inhibitors by pyrene assay. Based on the chemical structure of the seven candidates, another batch of optimized compounds was generated by using the structure-based drug design technology of Atomwise, and one hit was picked by pyrene assay in the end. Interestingly, all the selected compounds showed the ability to constrain actin polymerization This is in line with expectation since KAB is an actin polymerization inhibitor.

Moreover, these hit compounds are structurally similar to a group of compounds with demonstrated anti-cancer activities but without a known mode of action. Thiazole derivatives have emerged as promising therapeutic targets for cancer therapy. Thiazoles are heterocyclic organic compounds that contain a five-membered ring with three carbon atoms, one sulfur atom, and one nitrogen atom. They have shown diverse biological activities, including anticancer properties, making them attractive

candidates for drug development [142, 143]. After two rounds of screening, eight thiazole-containing compounds were selected as potential actin binding inhibitors. Overall, the structural and functional character of these compounds presents an intriguing opportunity for further investigation.

6.2.2 The efficacy of the selected compounds on cell proliferation and migration

Normally, the proliferation assay is used to measure the rate of cell propagation it helps us understand how cancer cells respond to these chemical stimuli [144]. The scratch assay can provide evaluation of the compounds in cell migration or cell-to-cell interactions, and their influence on wound closure [145].

Interestingly, when the concentrations of the compounds were increased to 200µM, all the available compounds displayed strong effects on Hela cells, this concentration is enough to cause a 50% reduction in cell growth especially for compounds 2,3,4 and 5. Although the migration was not significantly inhibited by the compounds, the remaining wound area still showed positive possibilities for clinical efficacy.

As expected, the capacity of both proliferation and migration of Hela cells was inhibited by the selected compounds. For this reason, we strongly believe that after structural modification, they will have the possibility of becoming clinical drugs for cancer therapy.

6.2.3 The selected compounds impaired the cytoskeletal structure

Since malignant cells often exhibit a perturbed cytoskeleton and are especially dependent on cytoskeletal functions due to their uncontrolled migration and

inappropriate invasion [146], we observed the morphology of the cytoskeleton after compound treatment. Compared with the control, 24 h treatment with compounds 1, 4, and 6 displayed actin cytoskeleton disruption resulting in the formation of some small aggregates. More notably, the F-actin fibers were reorganized under compound 2 or 5 stimulation leading to longer, straighter filaments. The disassembled cytoskeleton accumulated around the nucleus and deposited as curly-shaped aggregates at the peri-nuclear region.

Undeniably, the selected compounds had an effect on the organization of the F-actin network, they could disrupt the distribution of the cytoskeleton, and thereby altered cell morphology.

6.2.4 Conclusion and outlook

In cooperation with Atomwise, eight actin binding compounds were identified as actin polymerization inhibitors. High-concentration treatment could inhibit the Hela cell proliferation and migration ability. The actin staining study revealed impairment of the cytoskeletal structure with the stimulation of the compounds. Coupled with the presence of a similar anti-cancer thiazole structure, we speculated that these candidates had favorable drug-like properties and their chemical structure of them served as a guide for further drug discovery against malignancy.

References

7. References

1. Gunning, P.W., et al., *The evolution of compositionally and functionally distinct actin filaments.* J Cell Sci, 2015. **128**(11): p. 2009-19.
2. Williams, T.D. and A. Rousseau, *Actin dynamics in protein homeostasis.* Biosci Rep, 2022. **42**(9).
3. Dominguez, R. and K.C. Holmes, *Actin structure and function.* Annu Rev Biophys, 2011. **40**: p. 169-86.
4. Moraczewska, J., et al., *The DNase-I binding loop of actin may play a role in the regulation of actin-myosin interaction by tropomyosin/troponin.* J Biol Chem, 2004. **279**(30): p. 31197-204.
5. Pivovarova, A.V., S.Y. Khaitlina, and D.I. Levitsky, *Specific cleavage of the DNase-I binding loop dramatically decreases the thermal stability of actin.* Febs j, 2010. **277**(18): p. 3812-22.
6. Squire, J., *Special Issue: The Actin-Myosin Interaction in Muscle: Background and Overview.* Int J Mol Sci, 2019. **20**(22).
7. Wang, H., R.C. Robinson, and L.D. Burtnick, *The structure of native G-actin.* Cytoskeleton (Hoboken), 2010. **67**(7): p. 456-65.
8. Carlier, M.F., *Actin polymerization and ATP hydrolysis.* Adv Biophys, 1990. **26**: p. 51-73.
9. Cooper, J.A., S.B. Walker, and T.D. Pollard, *Pyrene actin: documentation of the validity of a sensitive assay for actin polymerization.* J Muscle Res Cell Motil, 1983. **4**(2): p. 253-62.
10. Pollard, T.D., L. Blanchoin, and R.D. Mullins, *Molecular mechanisms controlling actin filament dynamics in nonmuscle cells.* Annu Rev Biophys Biomol Struct, 2000. **29**: p. 545-76.
11. Lappalainen, P., et al., *Biochemical and mechanical regulation of actin dynamics.* Nat Rev Mol Cell Biol, 2022. **23**(12): p. 836-852.
12. Revenu, C., et al., *The co-workers of actin filaments: from cell structures to signals.* Nat Rev Mol Cell Biol, 2004. **5**(8): p. 635-46.
13. Schaks, M., G. Giannone, and K. Rottner, *Actin dynamics in cell migration.* Essays Biochem, 2019. **63**(5): p. 483-495.
14. Zigmond, S.H., *Signal transduction and actin filament organization.* Curr Opin Cell Biol, 1996. **8**(1): p. 66-73.
15. Otterbein, L.R., P. Graceffa, and R. Dominguez, *The crystal structure of uncomplexed actin in the ADP state.* Science, 2001. **293**(5530): p. 708-11.
16. Görlich, D. and I.W. Mattaj, *Nucleocytoplasmic transport.* Science, 1996. **271**(5255): p. 1513-8.
17. Pemberton, L.F. and B.M. Paschal, *Mechanisms of receptor-mediated nuclear import and nuclear export.* Traffic, 2005. **6**(3): p. 187-98.
18. Black, B.E., et al., *DNA binding domains in diverse nuclear receptors function as nuclear export signals.* Curr Biol, 2001. **11**(22): p. 1749-58.

19.   Nishida, E., et al., *Cofilin is a component of intranuclear and cytoplasmic actin rods induced in cultured cells.* Proc Natl Acad Sci U S A, 1987. **84**(15): p. 5262-6.

20.   Wada, A., et al., *Nuclear export of actin: a novel mechanism regulating the subcellular localization of a major cytoskeletal protein.* Embo j, 1998. **17**(6): p. 1635-41.

21.   Pawłowski, R., et al., *An actin-regulated importin α/β-dependent extended bipartite NLS directs nuclear import of MRTF-A.* Embo j, 2010. **29**(20): p. 3448-58.

22.   dos Remedios, C.G., et al., *Actin binding proteins: regulation of cytoskeletal microfilaments.* Physiol Rev, 2003. **83**(2): p. 433-73.

23.   Pollard, T.D., *Actin and Actin-Binding Proteins.* Cold Spring Harb Perspect Biol, 2016. **8**(8).

24.   Witke, W., *The role of profilin complexes in cell motility and other cellular processes.* Trends Cell Biol, 2004. **14**(8): p. 461-9.

25.   Arber, S., et al., *Regulation of actin dynamics through phosphorylation of cofilin by LIM-kinase.* Nature, 1998. **393**(6687): p. 805-9.

26.   Glenney, J.R., Jr., et al., *F-actin binding and bundling properties of fimbrin, a major cytoskeletal protein of microvillus core filaments.* J Biol Chem, 1981. **256**(17): p. 9283-8.

27.   Zheng, B., et al., *Nuclear actin and actin-binding proteins in the regulation of transcription and gene expression.* Febs j, 2009. **276**(10): p. 2669-85.

28.   Olave, I.A., S.L. Reck-Peterson, and G.R. Crabtree, *Nuclear actin and actin-related proteins in chromatin remodeling.* Annu Rev Biochem, 2002. **71**: p. 755-81.

29.   Hurst, V., K. Shimada, and S.M. Gasser, *Nuclear Actin and Actin-Binding Proteins in DNA Repair.* Trends Cell Biol, 2019. **29**(6): p. 462-476.

30.   Castano, E., et al., *Actin complexes in the cell nucleus: new stones in an old field.* Histochem Cell Biol, 2010. **133**(6): p. 607-26.

31.   Bettinger, B.T., D.M. Gilbert, and D.C. Amberg, *Actin up in the nucleus.* Nat Rev Mol Cell Biol, 2004. **5**(5): p. 410-5.

32.   Chatterjee, N. and G.C. Walker, *Mechanisms of DNA damage, repair, and mutagenesis.* Environ Mol Mutagen, 2017. **58**(5): p. 235-263.

33.   Kuo, L.J. and L.X. Yang, *Gamma-H2AX - a novel biomarker for DNA double-strand breaks.* In Vivo, 2008. **22**(3): p. 305-9.

34.   Scully, R., et al., *DNA double-strand break repair-pathway choice in somatic mammalian cells.* Nat Rev Mol Cell Biol, 2019. **20**(11): p. 698-714.

35.   Aleksandrov, R., et al., *The Chromatin Response to Double-Strand DNA Breaks and Their Repair.* Cells, 2020. **9**(8).

36.   Krejci, L., et al., *Homologous recombination and its regulation.* Nucleic Acids Res, 2012. **40**(13): p. 5795-818.

37.   Heeke, A.L., et al., *Prevalence of Homologous Recombination-Related Gene Mutations Across Multiple Cancer Types.* JCO Precis Oncol, 2018. **2018**.

38. Weterings, E. and D.C. van Gent, *The mechanism of non-homologous end-joining: a synopsis of synapsis.* DNA Repair (Amst), 2004. **3**(11): p. 1425-35.

39. de Almeida, L.C., et al., *DNA damaging agents and DNA repair: From carcinogenesis to cancer therapy.* Cancer Genet, 2021. **252-253**: p. 6-24.

40. Ferrara, L., H. Parekh-Olmedo, and E.B. Kmiec, *Enhanced oligonucleotide-directed gene targeting in mammalian cells following treatment with DNA damaging agents.* Exp Cell Res, 2004. **300**(1): p. 170-9.

41. Brandsma, I. and D.C. Gent, *Pathway choice in DNA double strand break repair: observations of a balancing act.* Genome Integr, 2012. **3**(1): p. 9.

42. Andrin, C., et al., *A requirement for polymerized actin in DNA double-strand break repair.* Nucleus, 2012. **3**(4): p. 384-95.

43. Schrank, B.R., et al., *Nuclear ARP2/3 drives DNA break clustering for homology-directed repair.* Nature, 2018. **559**(7712): p. 61-66.

44. Nieto, M.A., *The snail superfamily of zinc-finger transcription factors.* Nat Rev Mol Cell Biol, 2002. **3**(3): p. 155-66.

45. Shih, J.Y. and P.C. Yang, *The EMT regulator slug and lung carcinogenesis.* Carcinogenesis, 2011. **32**(9): p. 1299-304.

46. Lambert, A.W. and R.A. Weinberg, *Linking EMT programmes to normal and neoplastic epithelial stem cells.* Nat Rev Cancer, 2021. **21**(5): p. 325-338.

47. Peinado, H., D. Olmeda, and A. Cano, *Snail, Zeb and bHLH factors in tumour progression: an alliance against the epithelial phenotype?* Nat Rev Cancer, 2007. **7**(6): p. 415-28.

48. Wang, Y., et al., *The Role of Snail in EMT and Tumorigenesis.* Curr Cancer Drug Targets, 2013. **13**(9): p. 963-972.

49. Thiery, J.P., *Epithelial-mesenchymal transitions in tumour progression.* Nat Rev Cancer, 2002. **2**(6): p. 442-54.

50. Adimoolam, S. and J.M. Ford, *p53 and regulation of DNA damage recognition during nucleotide excision repair.* DNA Repair (Amst), 2003. **2**(9): p. 947-54.

51. Smith, M.L. and Y.R. Seo, *p53 regulation of DNA excision repair pathways.* Mutagenesis, 2002. **17**(2): p. 149-56.

52. Menon, V. and L. Povirk, *Involvement of p53 in the repair of DNA double strand breaks: multifaceted Roles of p53 in homologous recombination repair (HRR) and non-homologous end joining (NHEJ).* Subcell Biochem, 2014. **85**: p. 321-36.

53. Kajita, M., K.N. McClinic, and P.A. Wade, *Aberrant expression of the transcription factors snail and slug alters the response to genotoxic stress.* Mol Cell Biol, 2004. **24**(17): p. 7559-66.

54. Gross, K.M., et al., *Loss of Slug Compromises DNA Damage Repair and Accelerates Stem Cell Aging in Mammary Epithelium.* Cell Rep, 2019. **28**(2): p. 394-407.e6.

55. Pollard, T.D., *Regulation of actin filament assembly by Arp2/3 complex and formins.* Annu Rev Biophys Biomol Struct, 2007. **36**: p. 451-77.

56. Dogterom, M. and G.H. Koenderink, *Actin-microtubule crosstalk in cell biology.* Nat Rev Mol Cell Biol, 2019. **20**(1): p. 38-54.

57. Fuchs, E. and K. Weber, *Intermediate filaments: structure, dynamics, function, and disease.* Annu Rev Biochem, 1994. **63**: p. 345-82.

58. Fenteany, G. and S. Zhu, *Small-molecule inhibitors of actin dynamics and cell motility.* Curr Top Med Chem, 2003. **3**(6): p. 593-616.

59. Menhofer, M.H., et al., *The actin targeting compound Chondramide inhibits breast cancer metastasis via reduction of cellular contractility.* PLoS One, 2014. **9**(11): p. e112542.

60. Benitez-King, G., et al., *The neuronal cytoskeleton as a potential therapeutical target in neurodegenerative diseases and schizophrenia.* Curr Drug Targets CNS Neurol Disord, 2004. **3**(6): p. 515-33.

61. Roopnarine, O. and D.D. Thomas, *Mechanistic analysis of actin-binding compounds that affect the kinetics of cardiac myosin-actin interaction.* J Biol Chem, 2021. **296**: p. 100471.

62. Gronewold, T.M., et al., *Effects of rhizopodin and latrunculin B on the morphology and on the actin cytoskeleton of mammalian cells.* Cell Tissue Res, 1999. **295**(1): p. 121-9.

63. Bubb, M.R., et al., *Effects of jasplakinolide on the kinetics of actin polymerization. An explanation for certain in vivo observations.* J Biol Chem, 2000. **275**(7): p. 5163-70.

64. Morgan, S., et al., *The cost of drug development: a systematic review.* Health Policy, 2011. **100**(1): p. 4-17.

65. Carpenter, K.A. and X. Huang, *Machine Learning-based Virtual Screening and Its Applications to Alzheimer's Drug Discovery: A Review.* Curr Pharm Des, 2018. **24**(28): p. 3347-3358.

66. Stafford, K.A., et al., *AtomNet PoseRanker: Enriching ligand pose quality for dynamic proteins in virtual high-throuput screens.* Journal of Chemical Information and Modeling, 2022. **62**(5): p. 1178-1189.

67. Carpenter, K.A. and X. Huang, *Machine learning-based virtual screening and its applications to Alzheimer's drug discovery: a review.* Current pharmaceutical design, 2018. **24**(28): p. 3347-3358.

68. Wallach, I., M. Dzamba, and A. Heifets, *AtomNet: a deep convolutional neural network for bioactivity prediction in structure-based drug discovery.* arXiv preprint arXiv:1510.02855, 2015.

69. Wada, S., et al., *Actin-binding specificity of marine macrolide toxins, mycalolide B and kabiramide D.* J Biochem, 1998. **123**(5): p. 946-52.

70. Tanaka, J., et al., *Biomolecular mimicry in the actin cytoskeleton: mechanisms underlying the cytotoxicity of kabiramide C and related macrolides.* Proc Natl Acad Sci U S A, 2003. **100**(24): p. 13851-6.

71. Ryall, K.A. and A.C. Tan, *Systems biology approaches for advancing the discovery of effective drug combinations.* Journal of cheminformatics, 2015. **7**(1): p. 1-15.

72. Pomeroy, A.E., et al., *Drug independence and the curability of cancer by combination chemotherapy.* Trends in Cancer, 2022.

73.   Kadzik, R.S., K.E. Homa, and D.R. Kovar, *F-actin cytoskeleton network self-organization through competition and cooperation.* Annual review of cell and developmental biology, 2020. **36**: p. 35-60.

74.   Lehtimäki, J., M. Hakala, and P. Lappalainen, *Actin filament structures in migrating cells.* The Actin Cytoskeleton, 2017: p. 123-152.

75.   Fife, C.M., J.A. McCarroll, and M. Kavallaris, *Movers and shakers: cell cytoskeleton in cancer metastasis.* British journal of pharmacology, 2014. **171**(24): p. 5507-5523.

76.   Chen, C., et al., *Complex roles of the actin-binding protein Girdin/GIV in DNA damage-induced apoptosis of cancer cells.* Cancer science, 2020. **111**(11): p. 4303-4317.

77.   Hurst, V., et al., *Cytoskeleton integrity influences XRCC1 and PCNA dynamics at DNA damage.* Molecular Biology of the Cell, 2021. **32**(20): p. br6.

78.   Mering, C.v., et al., *STRING: a database of predicted functional associations between proteins.* Nucleic acids research, 2003. **31**(1): p. 258-261.

79.   Chen, Q. and T.D. Pollard, *Actin filament severing by cofilin is more important for assembly than constriction of the cytokinetic contractile ring.* Journal of Cell Biology, 2011. **195**(3): p. 485-498.

80.   Kotila, T., et al., *Mechanism of synergistic actin filament pointed end depolymerization by cyclase-associated protein and cofilin.* Nature Communications, 2019. **10**(1): p. 5320.

81.   Nakamura, F., et al., *Structural basis of filamin A functions.* The Journal of cell biology, 2007. **179**(5): p. 1011-1025.

82.   Rajan, S., D.S. Kudryashov, and E. Reisler, *Actin Bundles Dynamics and Architecture.* Biomolecules, 2023. **13**(3): p. 450.

83.   Morton, W.M., K.R. Ayscough, and P.J. McLaughlin, *Latrunculin alters the actin-monomer subunit interface to prevent polymerization.* Nature cell biology, 2000. **2**(6): p. 376-378.

84.   Bubb, M.R., et al., *Jasplakinolide, a cytotoxic natural product, induces actin polymerization and competitively inhibits the binding of phalloidin to F-actin.* Journal of Biological Chemistry, 1994. **269**(21): p. 14869-14871.

85.   Hemavathy, K., et al., *Human Slug is a repressor that localizes to sites of active transcription.* Molecular and cellular biology, 2000. **20**(14): p. 5087-5095.

86.   Chang, C.-Y., J.-D. Leu, and Y.-J. Lee, *The actin depolymerizing factor (ADF)/cofilin signaling pathway and DNA damage responses in cancer.* International journal of molecular sciences, 2015. **16**(2): p. 4095-4120.

87.   Norbury, C.J. and B. Zhivotovsky, *DNA damage-induced apoptosis.* Oncogene, 2004. **23**(16): p. 2797-2808.

88.   Kaina, B., *DNA damage-triggered apoptosis: critical role of DNA repair, double-strand breaks, cell proliferation and signaling.* Biochemical pharmacology, 2003. **66**(8): p. 1547-1554.

89.   Chabner, B.A. and T.G. Roberts Jr, *Chemotherapy and the war on cancer.* Nature Reviews Cancer, 2005. **5**(1): p. 65-72.

90. Müller, I., et al., *Effect of concentration on the cytotoxic mechanism of doxorubicin—apoptosis and oxidative DNA damage.* Biochemical and biophysical research communications, 1997. **230**(2): p. 254-257.

91. Rivankar, S., *An overview of doxorubicin formulations in cancer therapy.* Journal of cancer research and therapeutics, 2014. **10**(4): p. 853-858.

92. Carvalho, C., et al., *Doxorubicin: the good, the bad and the ugly effect.* Current medicinal chemistry, 2009. **16**(25): p. 3267-3285.

93. Sinha, R.P. and D.-P. Häder, *UV-induced DNA damage and repair: a review.* Photochemical & Photobiological Sciences, 2002. **1**(4): p. 225-236.

94. Rastogi, R.P., et al., *Molecular mechanisms of ultraviolet radiation-induced DNA damage and repair.* Journal of nucleic acids, 2010. **2010**.

95. Yu, S.-L. and S.-K. Lee, *Ultraviolet radiation: DNA damage, repair, and human disorders.* Molecular & Cellular Toxicology, 2017. **13**: p. 21-28.

96. Gross, K.M., et al., *Loss of slug compromises DNA damage repair and accelerates stem cell aging in mammary epithelium.* Cell Reports, 2019. **28**(2): p. 394-407. e6.

97. Pérez-Caro, M., et al., *Transcriptomal profiling of the cellular response to DNA damage mediated by Slug (Snai2).* British journal of cancer, 2008. **98**(2): p. 480-488.

98. Kuo, L.J. and L.-X. Yang, *γ-H2AX-a novel biomarker for DNA double-strand breaks.* In vivo, 2008. **22**(3): p. 305-309.

99. Rothkamm, K. and S. Horn, *gamma-H2AX as protein biomarker for radiation exposure.* Ann Ist Super Sanita, 2009. **45**(3): p. 265-71.

100. Dickey, J.S., et al., *H2AX: functional roles and potential applications.* Chromosoma, 2009. **118**: p. 683-692.

101. Ivashkevich, A., et al., *Use of the γ-H2AX assay to monitor DNA damage and repair in translational cancer research.* Cancer letters, 2012. **327**(1-2): p. 123-133.

102. Bastin-Shanower, S.A. and S.J. Brill, *Functional analysis of the four DNA binding domains of replication protein A. The role of RPA2 in ssDNA binding.* J Biol Chem, 2001. **276**(39): p. 36446-53.

103. Zou, L. and S.J. Elledge, *Sensing DNA damage through ATRIP recognition of RPA-ssDNA complexes.* Science, 2003. **300**(5625): p. 1542-8.

104. Wold, M.S., *Replication protein A: a heterotrimeric, single-stranded DNA-binding protein required for eukaryotic DNA metabolism.* Annu Rev Biochem, 1997. **66**: p. 61-92.

105. Zou, Y., et al., *Functions of human replication protein A (RPA): from DNA replication to DNA damage and stress responses.* J Cell Physiol, 2006. **208**(2): p. 267-73.

106. Bochkareva, E., et al., *The RPA32 subunit of human replication protein A contains a single-stranded DNA-binding domain.* J Biol Chem, 1998. **273**(7): p. 3932-6.

107. Pfitzer, L., et al., *Targeting actin inhibits repair of doxorubicin-induced DNA damage: a novel therapeutic approach for combination therapy.* Cell death & disease, 2019. **10**(4): p. 302.

108. Adler, J. and I. Parmryd, *Quantifying colocalization by correlation: the Pearson correlation coefficient is superior to the Mander's overlap coefficient.* Cytometry A, 2010. **77**(8): p. 733-42.

109. Ratner, B., *The correlation coefficient: Its values range between +1/−1, or do they?* Journal of Targeting, Measurement and Analysis for Marketing, 2009. **17**(2): p. 139-142.

110. Zagelbaum, J., et al., *Multiscale reorganization of the genome following DNA damage facilitates chromosome translocations via nuclear actin polymerization.* Nat Struct Mol Biol, 2023. **30**(1): p. 99-106.

111. Belin, B.J., T. Lee, and R.D. Mullins, *Correction: DNA damage induces nuclear actin filament assembly by Formin-2 and Spire-1/2 that promotes efficient DNA repair.* Elife, 2015. **4**.

112. Hyrskyluoto, A. and M.K. Vartiainen, *Regulation of nuclear actin dynamics in development and disease.* Curr Opin Cell Biol, 2020. **64**: p. 18-24.

113. Tanaka, J., et al., *Biomolecular mimicry in the actin cytoskeleton: mechanisms underlying the cytotoxicity of kabiramide C and related macrolides.* Proceedings of the National Academy of Sciences, 2003. **100**(24): p. 13851-13856.

114. Tetlow, D.J., S.J. Winder, and C. Aïssa, *The synthesis and biological evaluation of a kabiramide C fragment modified with a WH2 consensus actin-binding motif as a potential disruptor of the actin cytoskeleton.* Chemical Communications, 2015. **52**(4): p. 807-810.

115. Pollard, T.D. and J.A. Cooper, *Actin and actin-binding proteins. A critical evaluation of mechanisms and functions.* Annu Rev Biochem, 1986. **55**: p. 987-1035.

116. Causier, B. and B. Davies, *Analysing protein-protein interactions with the yeast two-hybrid system.* Plant Mol Biol, 2002. **50**(6): p. 855-70.

117. Yang, M., Z. Wu, and S. Fields, *Protein-peptide interactions analyzed with the yeast two-hybrid system.* Nucleic Acids Res, 1995. **23**(7): p. 1152-6.

118. Gietz, R.D., et al., *Identification of proteins that interact with a protein of interest: applications of the yeast two-hybrid system.* Mol Cell Biochem, 1997. **172**(1-2): p. 67-79.

119. Peche, V., et al., *CAP2, cyclase-associated protein 2, is a dual compartment protein.* Cell Mol Life Sci, 2007. **64**(19-20): p. 2702-15.

120. Aspit, L., et al., *CAP2 mutation leads to impaired actin dynamics and associates with supraventricular tachycardia and dilated cardiomyopathy.* J Med Genet, 2019. **56**(4): p. 228-235.

121. Svitkina, T., *The Actin Cytoskeleton and Actin-Based Motility.* Cold Spring Harb Perspect Biol, 2018. **10**(1).

122. Kustermans, G., J. Piette, and S. Legrand-Poels, *Actin-targeting natural compounds as tools to study the role of actin cytoskeleton in signal transduction.* Biochem Pharmacol, 2008. **76**(11): p. 1310-22.

123. Wakatsuki, T., et al., *Effects of cytochalasin D and latrunculin B on mechanical properties of cells.* J Cell Sci, 2001. **114**(Pt 5): p. 1025-36.

124. Holzinger, A., *Jasplakinolide: an actin-specific reagent that promotes actin polymerization.* Methods Mol Biol, 2009. **586**: p. 71-87.

125. Emadi Baygi, M., et al., *Slug/SNAI2 regulates cell proliferation and invasiveness of metastatic prostate cancer cell lines.* Tumour Biol, 2010. **31**(4): p. 297-307.

126. Oliveras-Ferraros, C., et al., *Epithelial-to-mesenchymal transition (EMT) confers primary resistance to trastuzumab (Herceptin).* Cell Cycle, 2012. **11**(21): p. 4020-32.

127. Pérez-Mancera, P.A., et al., *SLUG in cancer development.* Oncogene, 2005. **24**(19): p. 3073-3082.

128. Smyth, M.J., et al., *Combination cancer immunotherapies tailored to the tumour microenvironment.* Nat Rev Clin Oncol, 2016. **13**(3): p. 143-58.

129. Werner, H.M., G.B. Mills, and P.T. Ram, *Cancer Systems Biology: a peek into the future of patient care?* Nat Rev Clin Oncol, 2014. **11**(3): p. 167-76.

130. Urruticoechea, A., et al., *Recent advances in cancer therapy: an overview.* Curr Pharm Des, 2010. **16**(1): p. 3-10.

131. Gustafson, D.L., A.L. Merz, and M.E. Long, *Pharmacokinetics of combined doxorubicin and paclitaxel in mice.* Cancer Lett, 2005. **220**(2): p. 161-9.

132. Xin, Y., et al., *Demethoxycurcumin in combination with ultraviolet radiation B induces apoptosis through the mitochondrial pathway and caspase activation in A431 and HaCaT cells.* Tumour Biol, 2017. **39**(6): p. 1010428317706216.

133. Friedberg, E.C., *DNA damage and repair.* Nature, 2003. **421**(6921): p. 436-440.

134. Giglia-Mari, G., A. Zotter, and W. Vermeulen, *DNA damage response.* Cold Spring Harb Perspect Biol, 2011. **3**(1): p. a000745.

135. Jackson, S.P. and J. Bartek, *The DNA-damage response in human biology and disease.* Nature, 2009. **461**(7267): p. 1071-8.

136. Hoeijmakers, J.H., *DNA damage, aging, and cancer.* N Engl J Med, 2009. **361**(15): p. 1475-85.

137. Moyret-Lalle, C., et al., *Role of EMT in the DNA damage response, double-strand break repair pathway choice and its implications in cancer treatment.* Cancer Sci, 2022. **113**(7): p. 2214-2223.

138. Caridi, C.P., et al., *Nuclear actin filaments in DNA repair dynamics.* Nat Cell Biol, 2019. **21**(9): p. 1068-1077.

139. Garinis, G.A., et al., *Transcriptome analysis reveals cyclobutane pyrimidine dimers as a major source of UV-induced DNA breaks.* Embo j, 2005. **24**(22): p. 3952-62.

140. Kristó, I., et al., *Actin, actin-binding proteins, and actin-related proteins in the nucleus.* Histochem Cell Biol, 2016. **145**(4): p. 373-88.

141. Shen, J. and C.A. Nicolaou, *Molecular property prediction: recent trends in the era of artificial intelligence.* Drug Discovery Today: Technologies, 2019. **32**: p. 29-36.

142. Zheng, S., et al., *Discovery of a series of thiazole derivatives as novel inhibitors of metastatic cancer cell migration and invasion.* ACS medicinal chemistry letters, 2013. **4**(2): p. 191-196.

143. Sharma, P.C., et al., *Thiazole-containing compounds as therapeutic targets for cancer therapy.* European journal of medicinal chemistry, 2020. **188**: p. 112016.

144. Adan, A., Y. Kiraz, and Y. Baran, *Cell Proliferation and Cytotoxicity Assays.* Curr Pharm Biotechnol, 2016. **17**(14): p. 1213-1221.

145. Liang, C.C., A.Y. Park, and J.L. Guan, *In vitro scratch assay: a convenient and inexpensive method for analysis of cell migration in vitro.* Nat Protoc, 2007. **2**(2): p. 329-33.

146. Hall, A., *The cytoskeleton and cancer.* Cancer Metastasis Rev, 2009. **28**(1-2): p. 5-14.

Appendix

8. Appendix

8.1 Supplementary

| Insert Identity	Frequency
3'-phosphoadenosine 5'-phosphosulfate synthase 1 (PAPSS1)	1
ribosome biogenesis protein BRX1 homolog (BRIX1)	1
chromosome 9 open reading frame 131 (C9orf131)	1
cofilin 2 (CFL2)	16
COP9 signalosome subunit 5 (COPS5)	8
cyclase associated actin cytoskeleton regulatory protein 2 (CAP2)	164
cysteine sulfinic acid decarboxylase (CSAD)	3
double zinc ribbon and ankyrin repeat domains 1 (DZANK1)	1
dual specificity phosphatase 5 (DUSP5)	3
endoplasmic reticulum lectin 1 (ERLEC1)	1
transcription and export complex 2 subunit (ENY2)	1
epidermal growth factor receptor pathway substrate 8 (EPS8)	1
F-box and WD repeat domain containing 7 (FBXW7)	1
gamma-aminobutyric acid type A receptor alpha4 subunit (GABRA4)	1
integrin subunit alpha 8 (ITGA8)	2
late endosomal/lysosomal adaptor, MAPK and MTOR activator 5 (LAMTOR5)	8
lysine acetyltransferase 14 (KAT14)	10
NLR family pyrin domain containing 1 (NLRP1)	13
nuclear receptor binding factor 2 (NRBF2)	2
phosphodiesterase 1C (PDE1C)	1
RAD51 associated protein 2 (RAD51AP2)	62
ribosomal protein L26 (RPL26)	1
snail family transcriptional repressor 2 (SNAI2)	1
SNAP associated protein (SNAPIN)	9
translation machinery associated 7 homolog (TMA7)	11
VHL binding protein 1 (VBP1)	3
zinc finger CCHC-type containing 4 (ZCCHC4)	2
zinc finger protein 148 (ZNF148)	3

Supplementary Table 8-1.1 Proteins screened out by the Matchmaker Gold yeast two hybrid system.

A

B
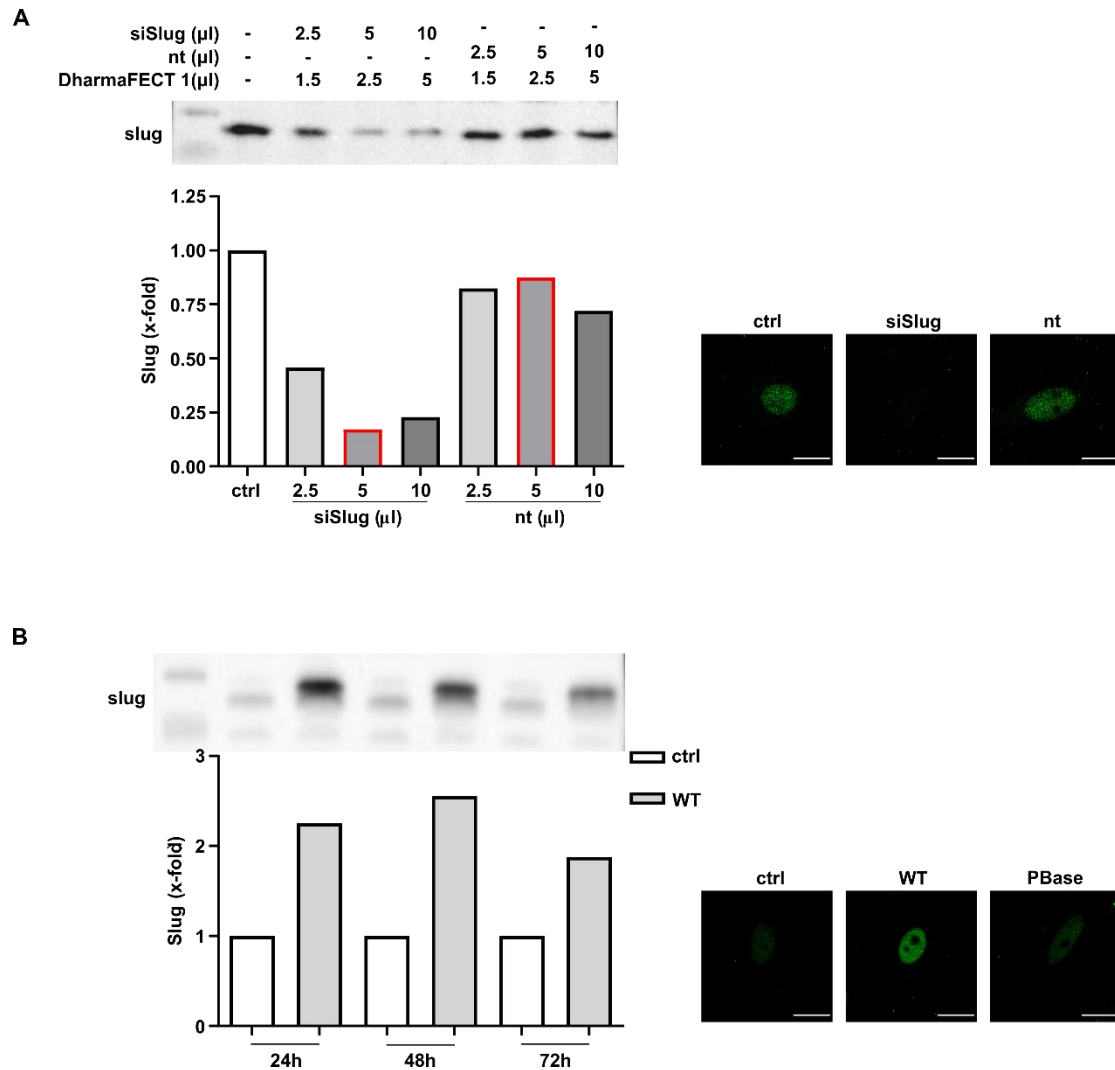
Supplementary Figure 8-1.2 Validation of transfection efficiency of knockdown and overexpression of slug.

(A) Knockdown efficiency test of transfection using DharmaFECT 1 reagent. Western blotting (left) demonstrated that 5 µl of siRNA or non-targeting control siRNA and 2.5 µl of DharmaFECT 1 reagent showed best the efficiency. The confocal images (right) indicated that knockdown of slug could significantly decrease the expression in nucleus.

(B) Overexpression efficiency test of transfection using lipofectamine™ 3000 reagents. Western blotting analysis (left) pointed out that the expression levels of the slug 48 h after transfection showed the best efficiency. Immunofluorescence confirmed that protein level was increased significantly following overexpression of slug in cells.
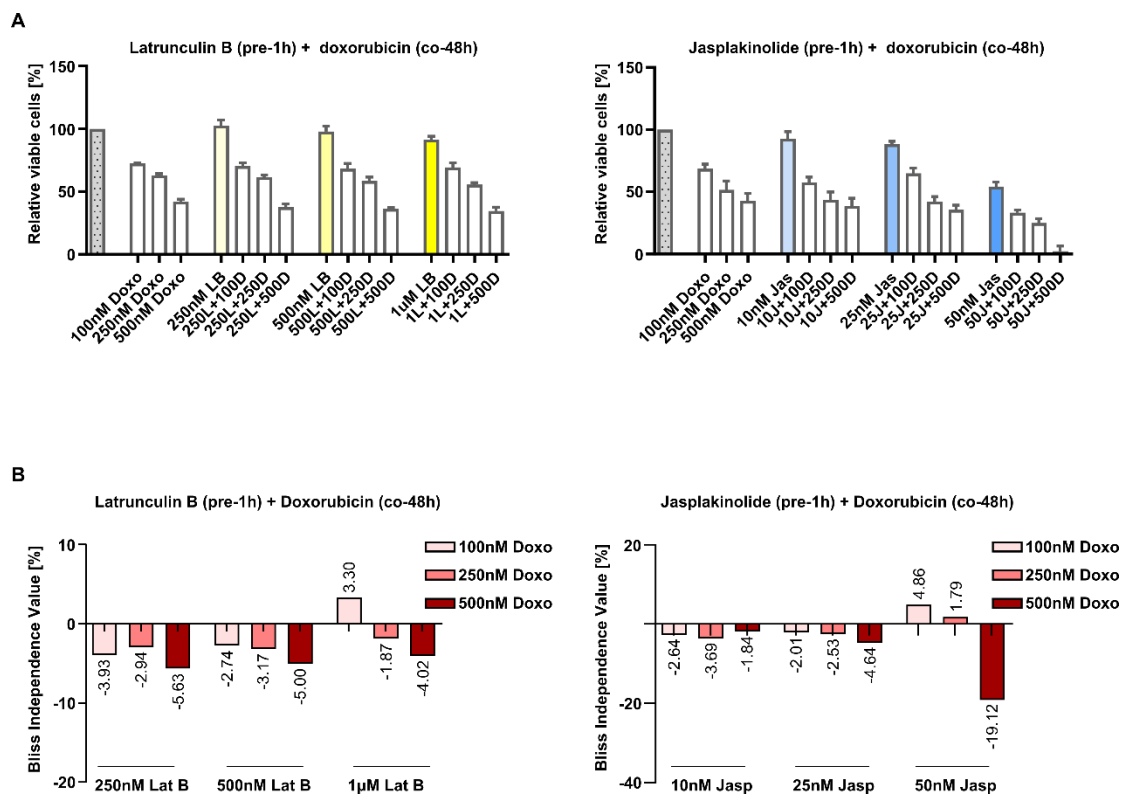
Supplementary Figure 8-1.3 Effects of drug combination treatment on cell viability in Hela cells.

(A) Actin binding compounds and doxo dose-dependently inhibited cellular metabolic activity in Hela. Cells were pre-treated with the indicated actin substances for 1 h and in combination with doxo, cell viability was determined by MTT assay after 48 h co-treatment. The percentage of viable cells is shown. (n=3, mean ± SEM)

(B) Bliss independence analysis of cell viability effect of dual-component model. Negative values represented synergistic potency. (n=3)
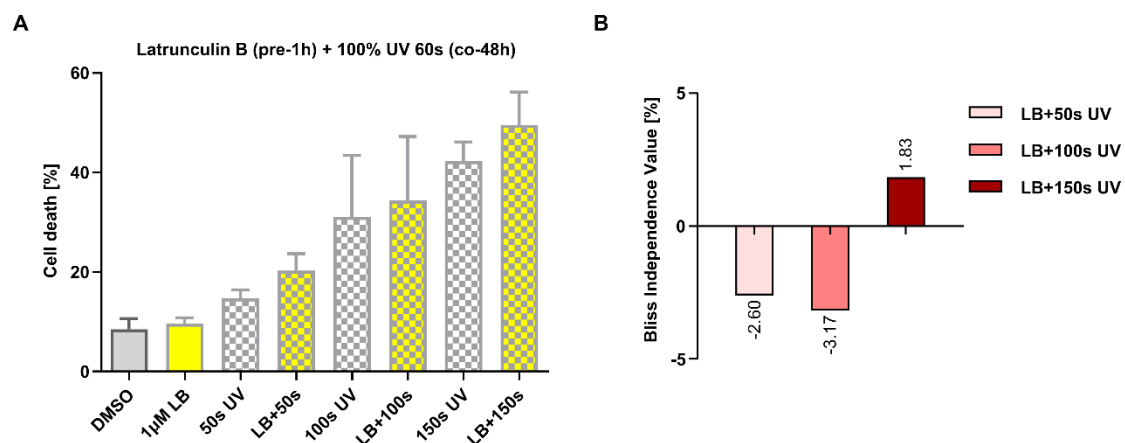
Supplementary Figure 8-1.4 Cell viability effect of Lat B-UVA model measured by PI assay.

(A) The combination of 1µM Lat B and UVA treatment acted synergistically. The cell viability was determined by propidium iodide (PI) staining after 48 h. (n=3, mean ± SEM)
(B) Bliss independence analysis of cell viability effects on the Lat B-UVA model. Positive values represented synergistic potency. (n=3)

pmCherry-C1 actin-3XNLS P2A mCherry   **Nuclear Actin-Chromobody TagGFP2**
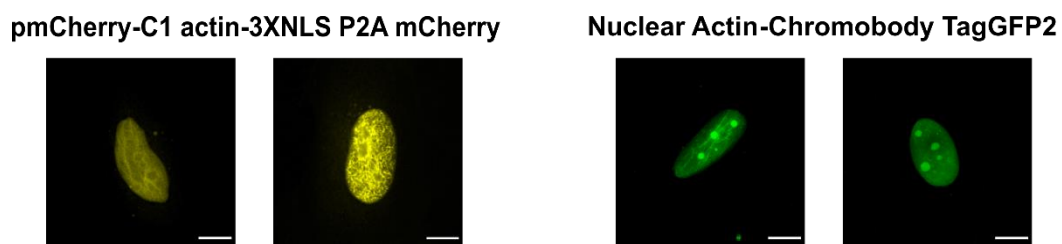
Supplementary Figure 8-1.5 The morphology of nuclear actin overexpressed with two different plasmids.

Hela cells were transfected with pmCherry-C1 actin-3XNLS P2A mCherry plasmid and Nuclear Actin-Chromobody TagGFP2 plasmid to visualize nuclear actin respectively. The representative images showed long actin filaments and short actin sticks or dots in the nucleus. Three different square regions of each nucleus were chosen for co-localization analysis.

8.2 Abbreviations

Abbreviation	Term
ABPs	actin binding proteins
ADP	adenosine diphosphate
AI	artificial intelligence
ARP	actin-related protein
ATP	adenosine triphosphate
BER	base excision repair
BRCA2	breast cancer type 2 susceptibility protein
CAP1	cyclase associated actin cytoskeleton regulatory protein 1
CFL2	cofilin 2
Co-IP	co-immunoprecipitation
DDR	DNA damage response
D-loop	displacement loop
DMSO	dimethyl sulfoxide
DSB	double-strand break
EMT	epithelial-mesenchymal transition
HR	homologous recombination
hSlug	human slug protein
HTS	high-throughput screening
IC50	half maximal inhibitory concentration
Jasp	jasplakinolide
KAB	kabiramide
Lat B	latrunculin B
ML	machine learning
N/C	nuclear-cytoplasmic
NABPs	nuclear actin binding proteins
NER	nucleotide excision repair
NES	nuclear export signal
NHEJ	non-homologous end joining
NLS	nuclear localization sequence
Pi	inorganic phosphate
PI	propidium iodide
RPA	replication protein A
SNAI2/slug	snail family transcriptional repressor 2
ssDNA	single-stranded DNA
Y2H	yeast two-hybrid screening system

List of abbreviations

8.3 Publications

AI-based computational screening for small molecular inhibitors of actin polymerization

Ling Zhuo, Ryan Pemberton, Denzil Bernard, Angelika M. Vollmar & Stefan Zahler

In preparation

The interaction of slug and actin in the DNA double-strand break repair

Ling Zhuo, Simone Moser, Angelika M. Vollmar, Stefan Zahler

In preparation

Turning the actin nucleating compound Miuraenamide into nucleation inhibitors

Shuaijun Wang, Maximilian Meixner, Lushuang Yu, <u>Ling Zhuo</u>, Lisa Karmann, Uli Kazmaier, Angelika M. Vollmar, Iris Antes, and Stefan Zahler

ACS Omega. 2021 Aug 18;6(34):22165-22172.

8.4 Acknowledgements

First and foremost, I am immensely grateful to my supervisor, Prof. Dr. Angelika M. Vollmar and Prof. Dr. Stefan Zahler, for their exceptional mentorship throughout this journey. Their expertise, patience, and unwavering support have been invaluable in shaping the direction of my research and guiding me through the challenges that arose along the way. I am indebted to them for their insightful feedback, constructive criticism, and constant motivation.

I extend my sincere appreciation to the members of my thesis committee, Prof. Dr. Stefan Zahler, Prof. Dr. Angelika Vollmar, Prof. Dr. Franz Bracher, Prof. Dr. Susanne Koch, Prof. Dr. Olivia Merkel, Prof. Dr. Ernst Wagner, for their valuable evaluation of my work. I am grateful for the time and effort they dedicated to reviewing and assessing my research.

My heartfelt gratitude goes to Dr. Simone Moser for initiating the interaction between the slug and actin project together with Prof. Dr. Zahler. Their positive cooperation and willingness to address problems are instrumental in the progress of this study. Special thanks go to Atomwise company, which provided advanced technology support essential to successfully completing the actin binding compound research.

I am extremely grateful to the China Scholarship Council (CSC) for their invaluable support and for providing me with the opportunity to pursue my Doctoral studies at LMU Munich. I am deeply indebted to the CSC for their unwavering support and the trust that has been placed in me, which has allowed me to embark on a fulfilling academic career in this beautiful city. The generous scholarship from the CSC has not only relieved the financial burden associated with my studies but has also provided me with the means to fully immerse myself in the academic environment at LMU Munich in Prof. Vollmar's group.